

Supporting Information to:

meso-Tetraphenyl-2-oxabacteriochlorins and
meso-Tetraphenyl-2,12/13-dioxabacteriochlorins

Junichi Ogikubo,[†] Eileen Meehan,[†]

James T. Engle,^{} Christopher J. Ziegler,^{*} and Christian Brückner^{†,*}*

Department of Chemistry, University of Connecticut, Storrs, CT 06269-3060,
United States.

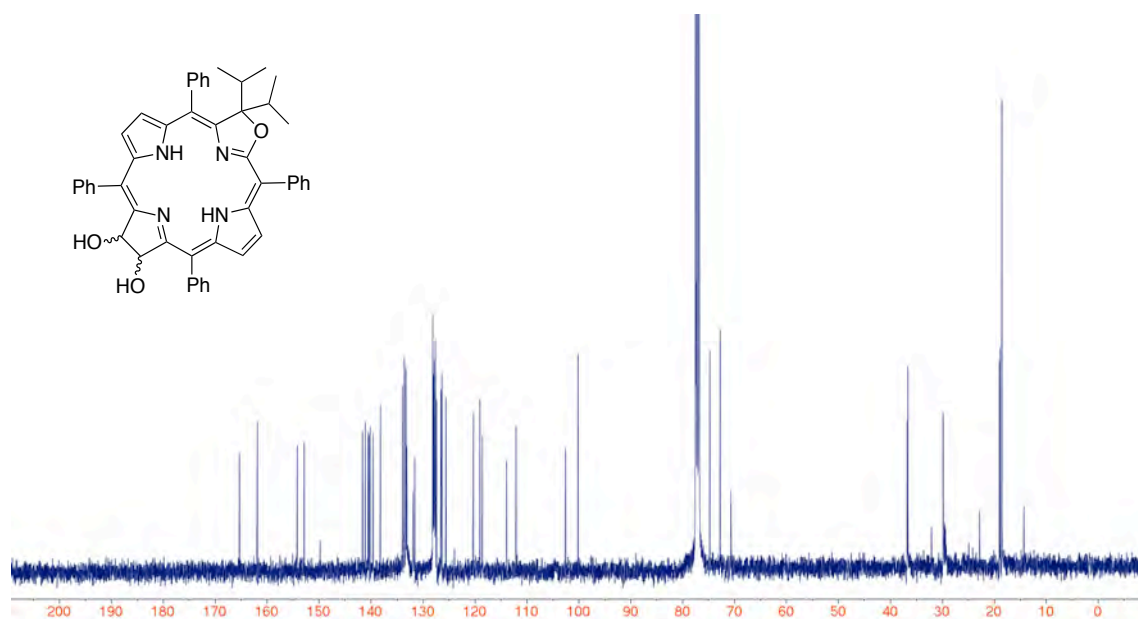
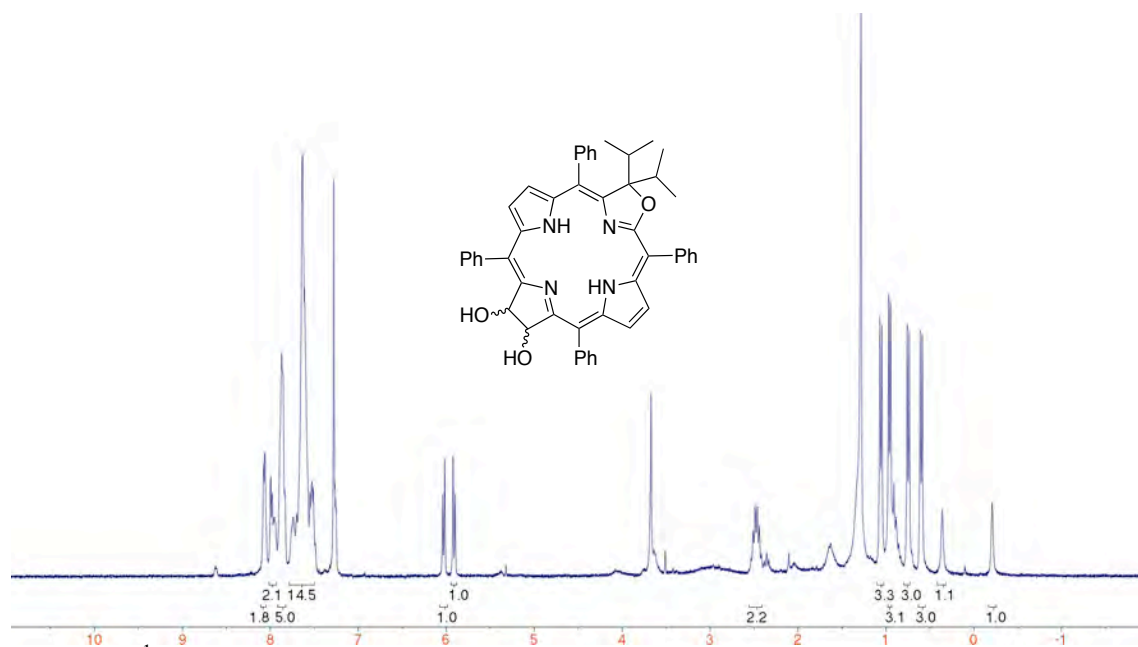
Department of Chemistry, University of Akron, Akron, OH 44325-3601, United
States.

Author to whom inquiries should be addressed to: c.bruckner@uconn.edu

Table of Contents:

Figure 1. ^1H NMR spectrum (400 CDCl_3 , CDCl_3) of 13	4
Figure 2. ^{13}C NMR spectrum (100 MHz, CDCl_3) of 13	4
Figure 3. UV-vis and fluorescence spectra of 13 (CH_2Cl_2)	5
Figure 4. FT-IR spectrum (neat, diffuse reflectance) of 13	5
Figure 5. ^1H NMR spectrum (400 MHz, CDCl_3) of 14-cis	6
Figure 6. ^{13}C NMR spectrum (100 MHz, CDCl_3) of 14-cis	6
Figure 7. UV-vis and fluorescence spectra of 14-cis (CH_2Cl_2)	7
Figure 8. FT-IR spectrum (neat, diffuse reflectance) of 14-cis	7
Figure 9. ^1H NMR spectrum (400 MHz, CDCl_3) of 15	8
Figure 10. ^{13}C NMR spectrum (100 MHz, CDCl_3) of 15	8
Figure 11. UV-vis and fluorescence spectra of 15 (CH_2Cl_2)	9
Figure 12. ^1H NMR spectrum (400 MHz, CDCl_3) of 17	9
Figure 13. ^{13}C NMR spectrum (100 MHz, CDCl_3) of 17	10
Figure 14. UV-vis and fluorescence spectra of 17 (CHCl_3)	10
Figure 15. ^1H NMR spectrum (400 MHz, CDCl_3) of 16-cis	11
Figure 16. ^{13}C NMR spectrum (100 MHz, CDCl_3) of 16-cis	11
Figure 17. UV-vis and fluorescence spectra of 16-cis (CH_2Cl_2)	12
Figure 18. FT-IR spectrum (neat, diffuse reflectance) of 16-cis	12
Figure 19. ^1H NMR spectrum (400 MHz, CDCl_3) of 16Zn-cis	13
Figure 20. ^{13}C NMR spectrum (100 MHz, CDCl_3) of 16Zn-cis	13
Figure 21. UV-vis and fluorescence spectra of 16Zn-cis (CH_2Cl_2)	14
Figure 22. FT-IR spectrum (neat, diffuse reflectance) of 16Zn-cis	14
Figure 23. ^1H NMR spectrum (400 MHz, CDCl_3) of 18-cis	15
Figure 24. ^{13}C NMR spectrum (100 MHz, CDCl_3) of 18-cis	15
Figure 25. UV-vis and fluorescence spectra of 18-cis (CH_2Cl_2)	16
Figure 26. FT-IR spectrum (neat, diffuse reflectance) of 18-cis	16
Figure 27. ^1H NMR spectrum (400 MHz, CDCl_3) of 19-cis	17
Figure 28. ^{13}C NMR spectrum (100 MHz, CDCl_3) of 19-cis	17
Figure 29. UV-vis and fluorescence spectra of 19-cis (CH_2Cl_2)	18
Figure 30. FT-IR spectrum (neat, diffuse reflectance) of 19-cis	18
Figure 31. ^1H NMR spectrum (400 MHz, CDCl_3) of 25 (mixture of all isomers+)	19

Figure 32. ^{13}C NMR spectrum (100 MHz, CDCl_3) of 23 (mixture of all isomers)	19
Figure 33. UV-vis spectrum of 23 (CH_2Cl_2 , mixture of all isomers)	20
Figure 34. ^1H NMR spectrum (400 MHz, CDCl_3) of 22-cis / trans (CH_2Cl_2), mixture, 3:2 favoring 22-cis)	20
Figure 35. ^{13}C NMR spectrum (100 MHz, CDCl_3) of 22-cis / trans (mixture, 3:2 favoring 22-cis)	21
Figure 36. UV-vis spectrum of 22-cis / trans (CH_2Cl_2 , mixture, 3:2 favoring 22-cis)	21
Figure 37. ^1H NMR spectrum (500 MHz, CDCl_3) of 24	22
Figure 38. ^{13}C NMR spectrum (100 MHz, CDCl_3) of 24	22
Figure 39. UV-vis spectrum of 24 (CH_2Cl_2)	23
Crystal Structure Report for 14-cis	24
Figure 40. ORTEP Representation of the crystal structure of 14-cis , side and top views. Hydrogen atoms and disorder removed for clarity.	25
Table S1. Crystal data and structure refinement for 14-cis .	40
Crystal Structure Report for 16-cis	27
Figure 41. ORTEP Representation of the crystal structure of 16-cis , side and top views. Hydrogen atoms and disorder removed for clarity.	28
Table S2. Crystal data and structure refinement for 16-cis	40
Crystal Structure Report for 16Zn-cis	30
Figure 42. ORTEP Representation of the crystal structure of 16Zn-cis , side and top views. Hydrogen atoms and disorder removed for clarity.	31
Table S3. Crystal data and structure refinement for 16Zn-cis	40
Crystal Structure Report for 23-trans-E	33
Figure 43. ORTEP Representation of the crystal structure of 22-trans-E , side and top views. Hydrogen atoms and disorder removed for clarity.	34
Table S4. Crystal data and structure refinement for 22-trans-E	40
Crystal Structure Report for 23-trans-Z	36
Figure 44. ORTEP Representation of the crystal structure of 23-trans-E , side and top views. Hydrogen atoms and disorder removed for clarity.	37
Table S5. Crystal data and structure refinement for 23-trans-E	40
Crystal Structure Report for 22-cis	39
Figure 45. ORTEP Representation of the crystal structure of 22-cis , side and top views. Hydrogen atoms and disorder removed for clarity.	40
Table S6. Crystal data and structure refinement for 22-cis .	41



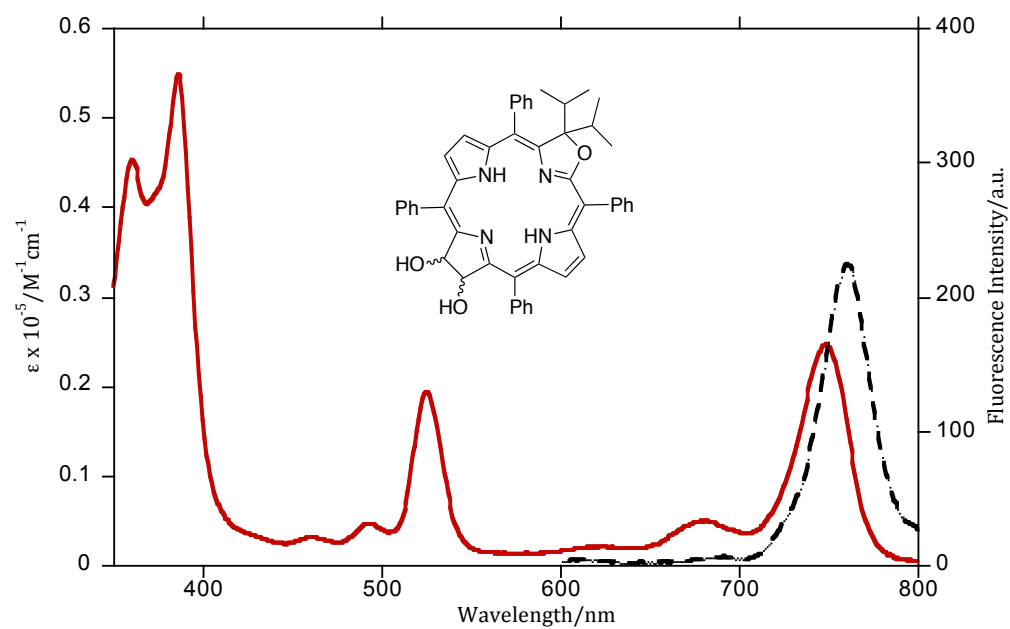


Figure 3. UV-vis (solid red trace) and fluorescence (broken black trace) spectra of **13** (CH_2Cl_2)

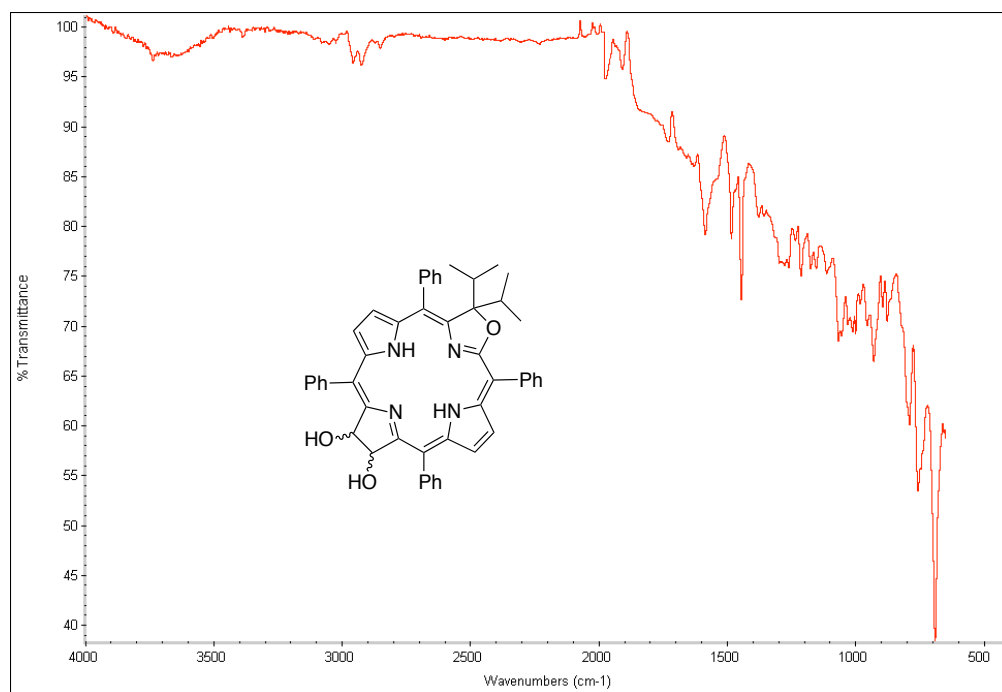


Figure 4. FT-IR spectrum (neat, diffuse reflectance) of **13**

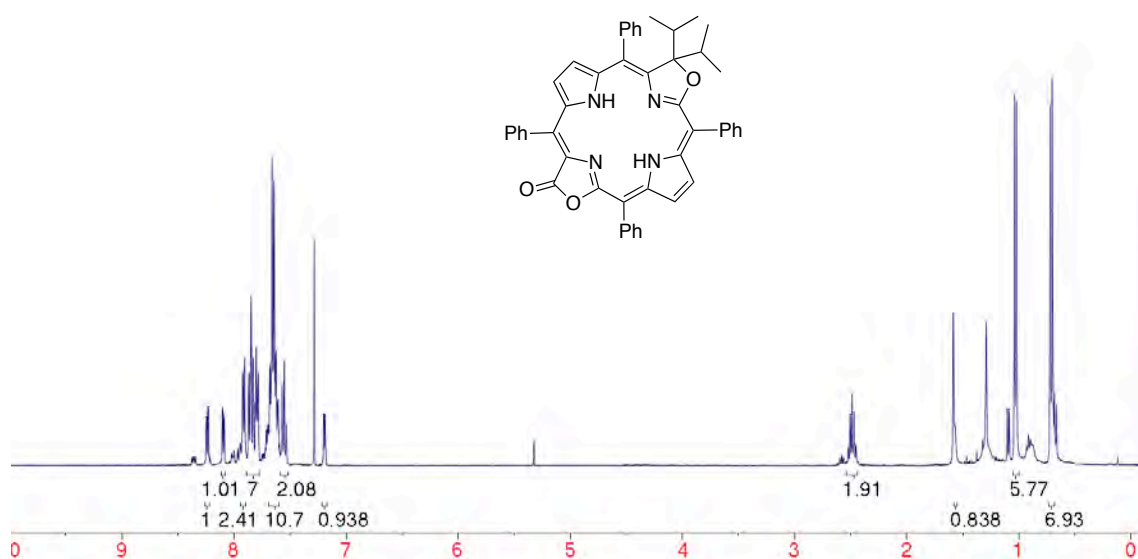


Figure 5. ¹H NMR spectrum (400 MHz, CDCl₃) of **14-cis**

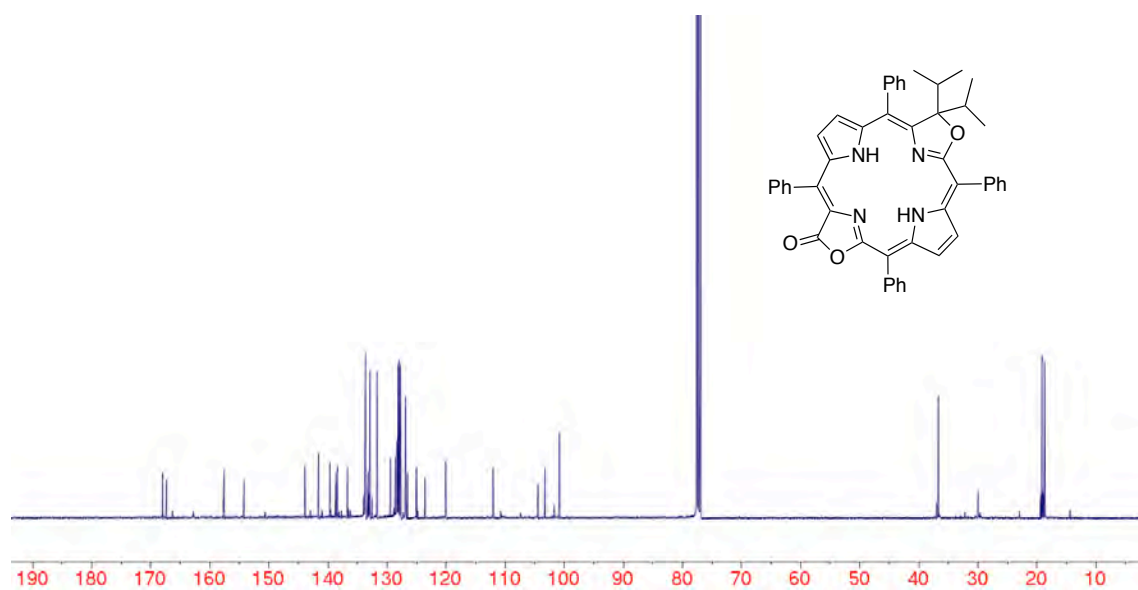


Figure 6. ¹³C NMR spectrum (100 MHz, CDCl₃) of **14-cis**

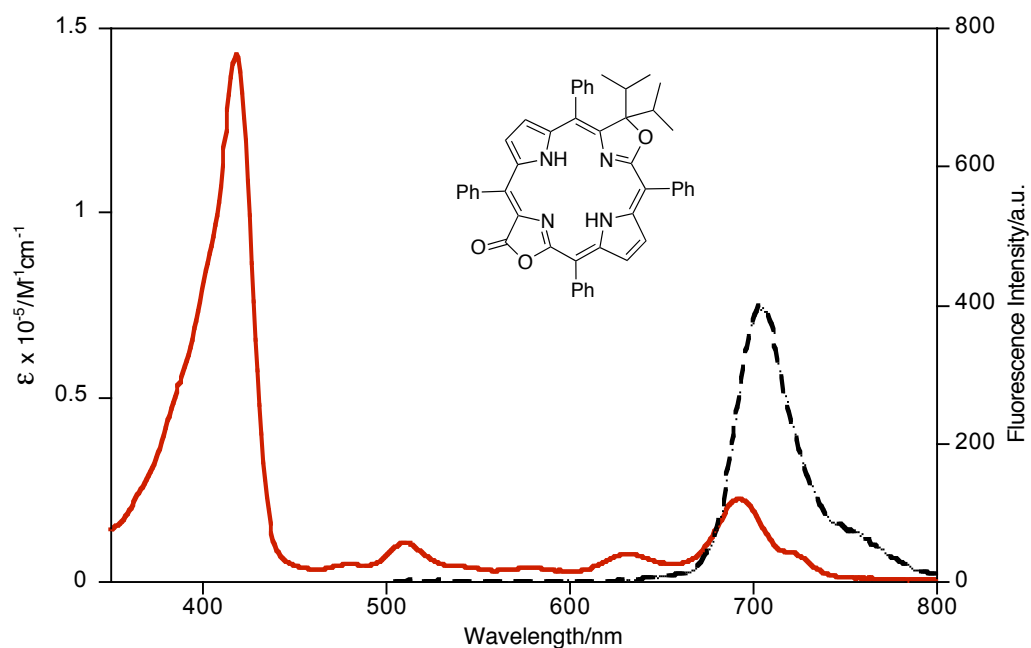


Figure 7. UV-vis (solid red trace) and fluorescence (broken black trace) spectra of **14-cis** (CH_2Cl_2)

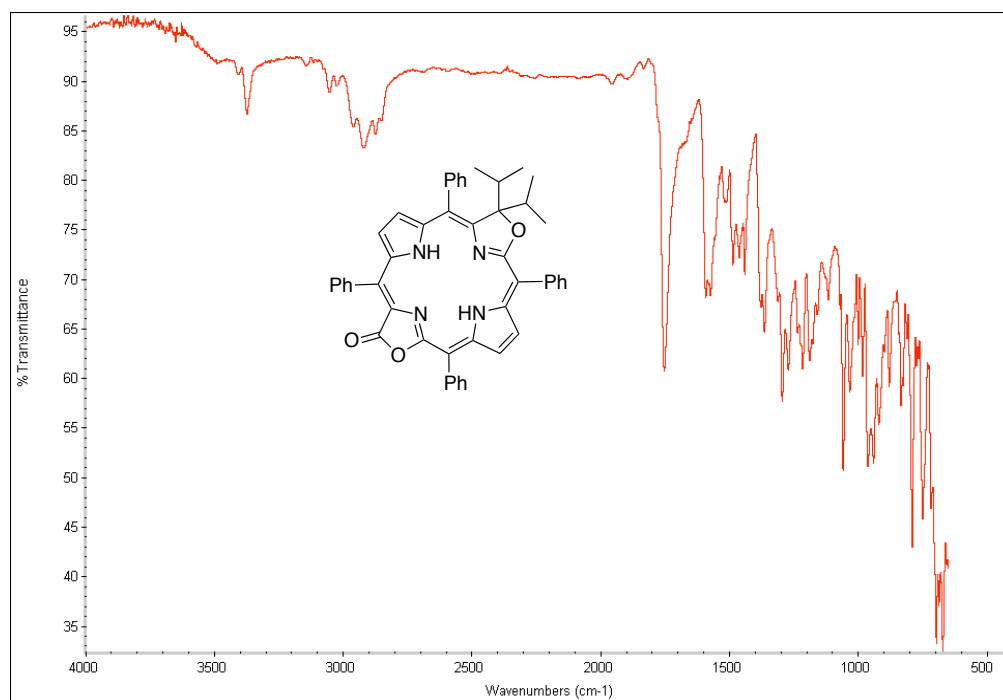


Figure 8. FT-IR spectrum (neat, diffuse reflectance) of **14-cis**

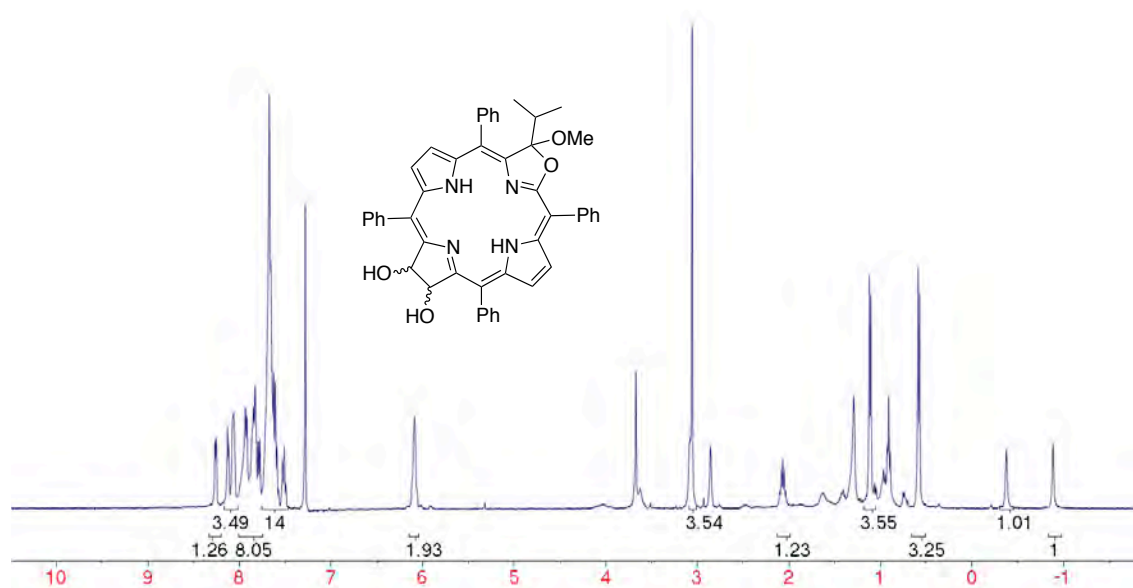


Figure 9. ^1H NMR spectrum (400 MHz, CDCl_3) of **15**

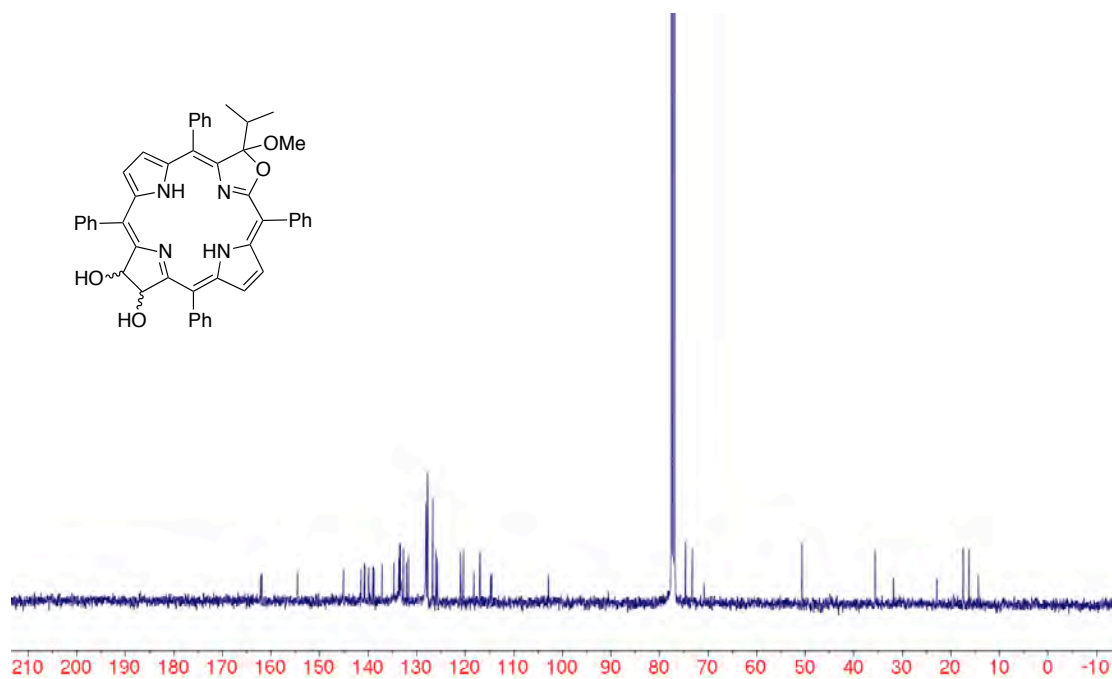


Figure 10. ^{13}C NMR spectrum (100 MHz, CDCl_3) of **15**

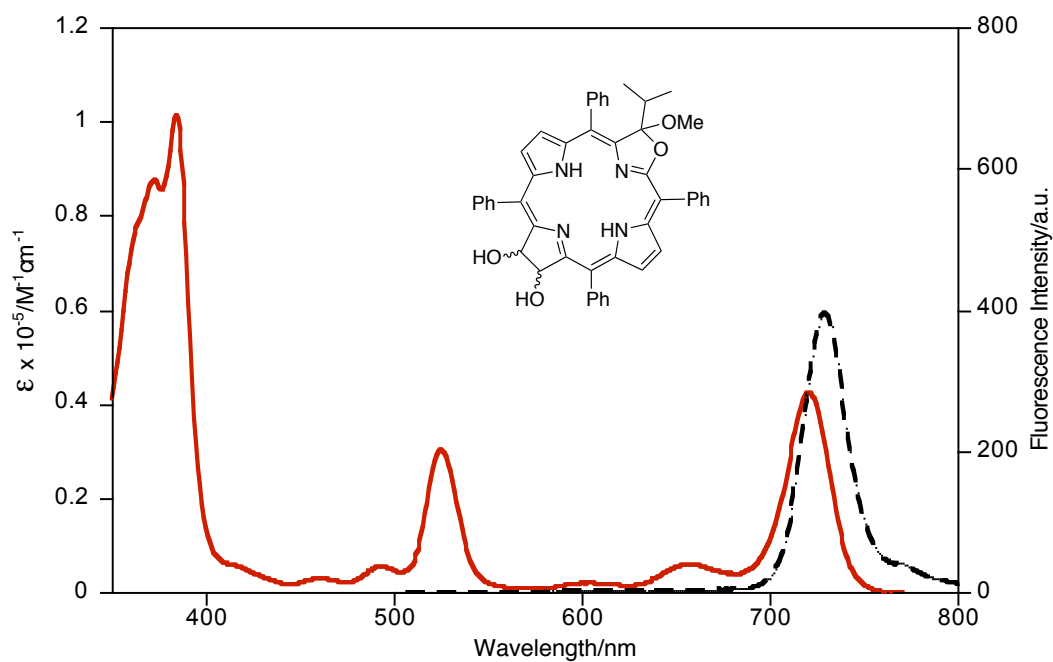


Figure 11. UV-vis (solid red trace) and fluorescence (broken black trace) spectra of **15** (CH_2Cl_2)

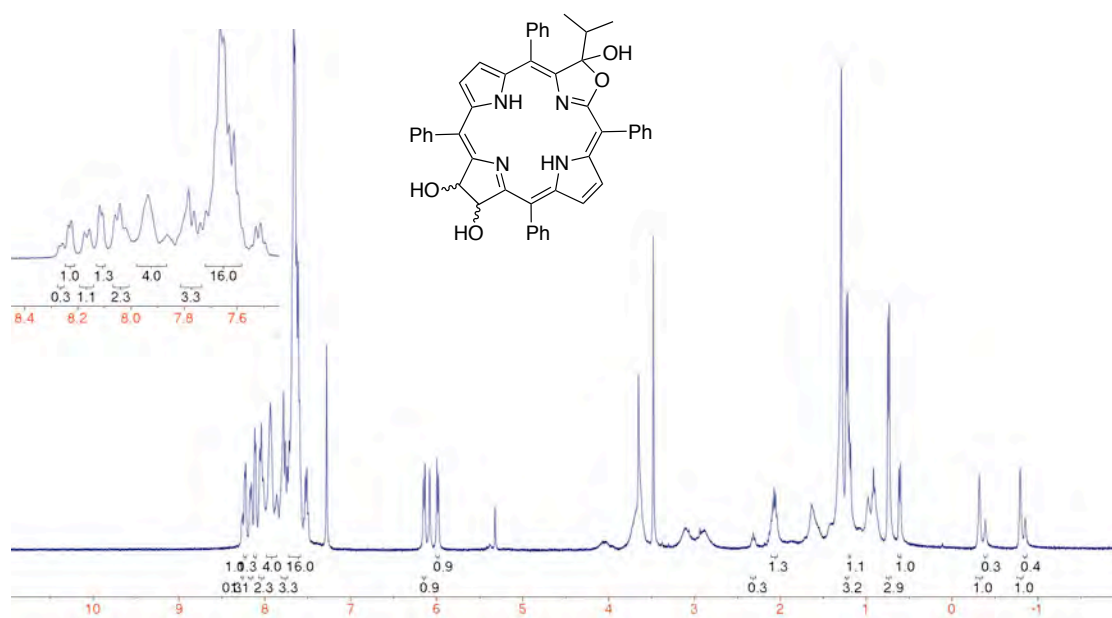


Figure 12. ^1H NMR spectrum (400 MHz, CDCl_3) of **17**

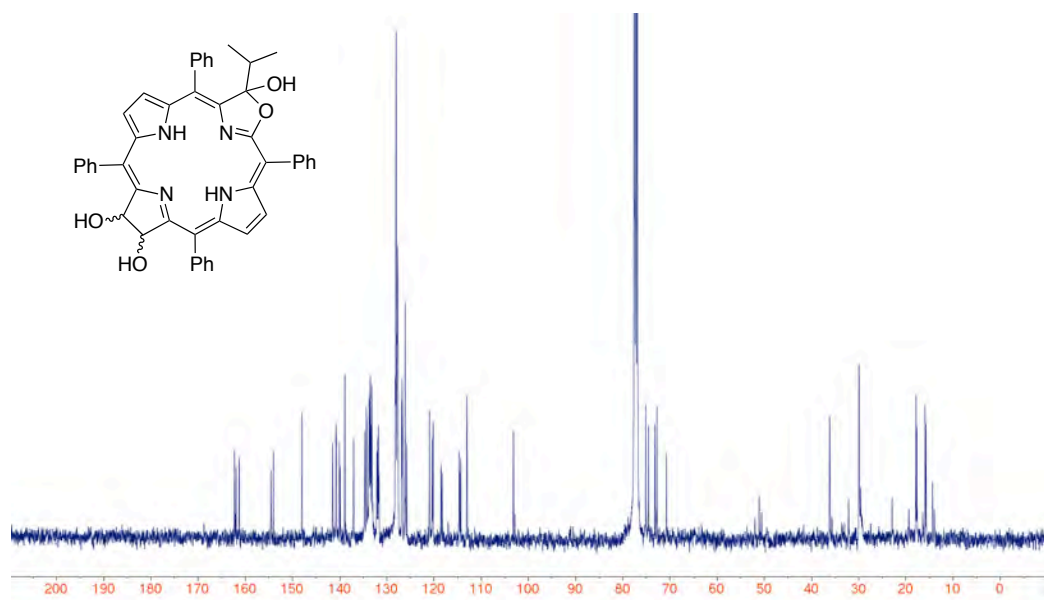


Figure 13. ^{13}C NMR spectrum (100 MHz, CDCl_3) of **17**

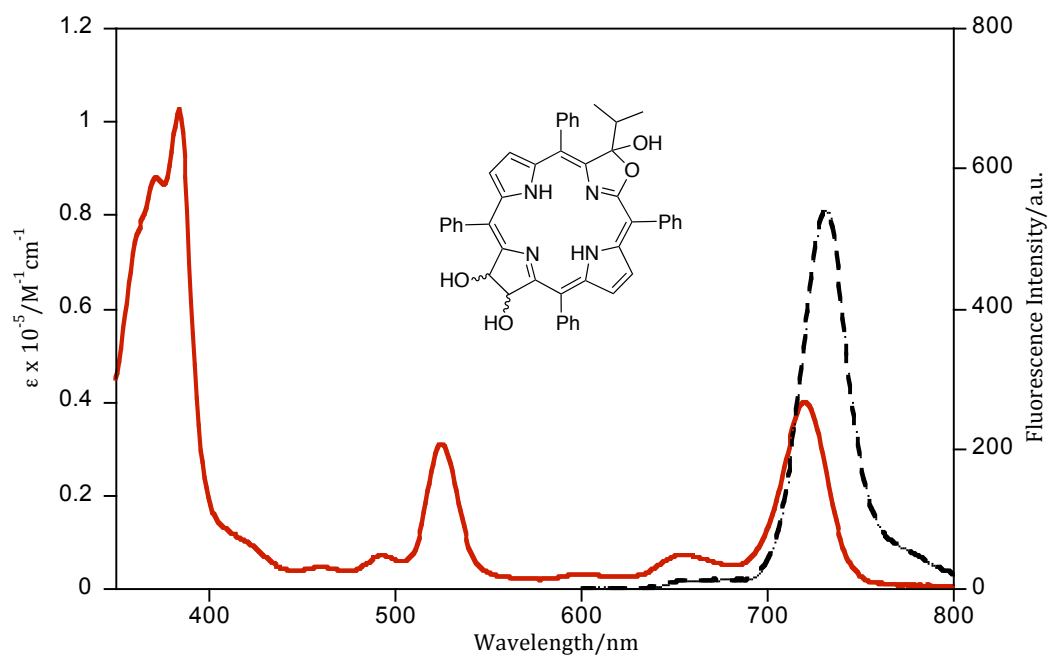


Figure 14. UV-vis (solid red trace) and fluorescence (broken black trace) spectra of **17** (CHCl_3)

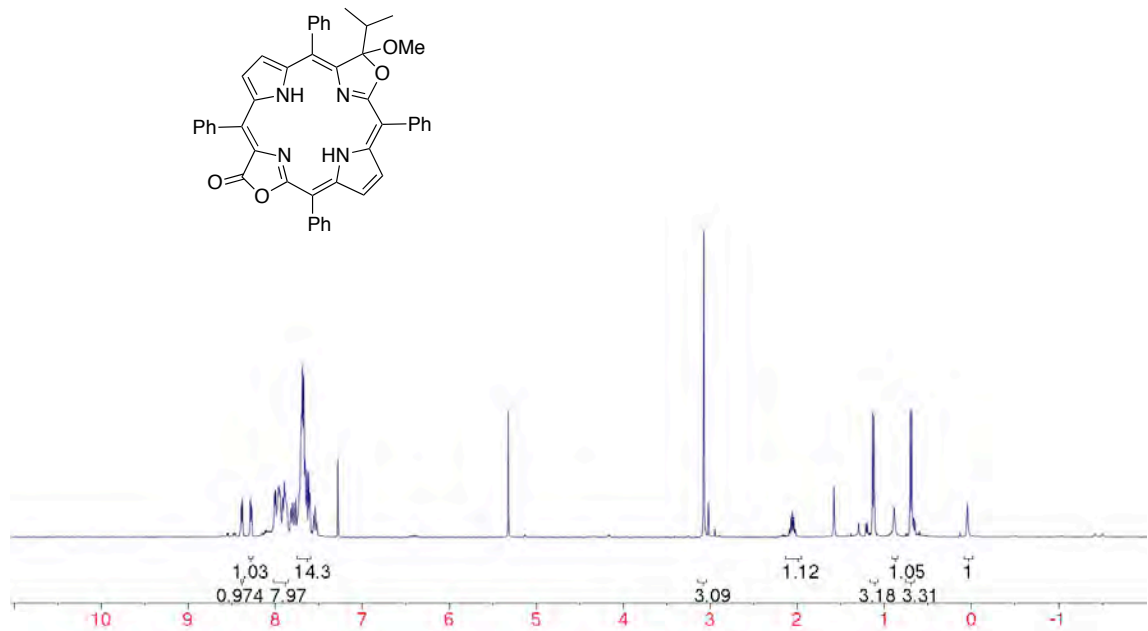


Figure 15. ^1H NMR spectrum (400 MHz, CDCl_3) of **16-cis**

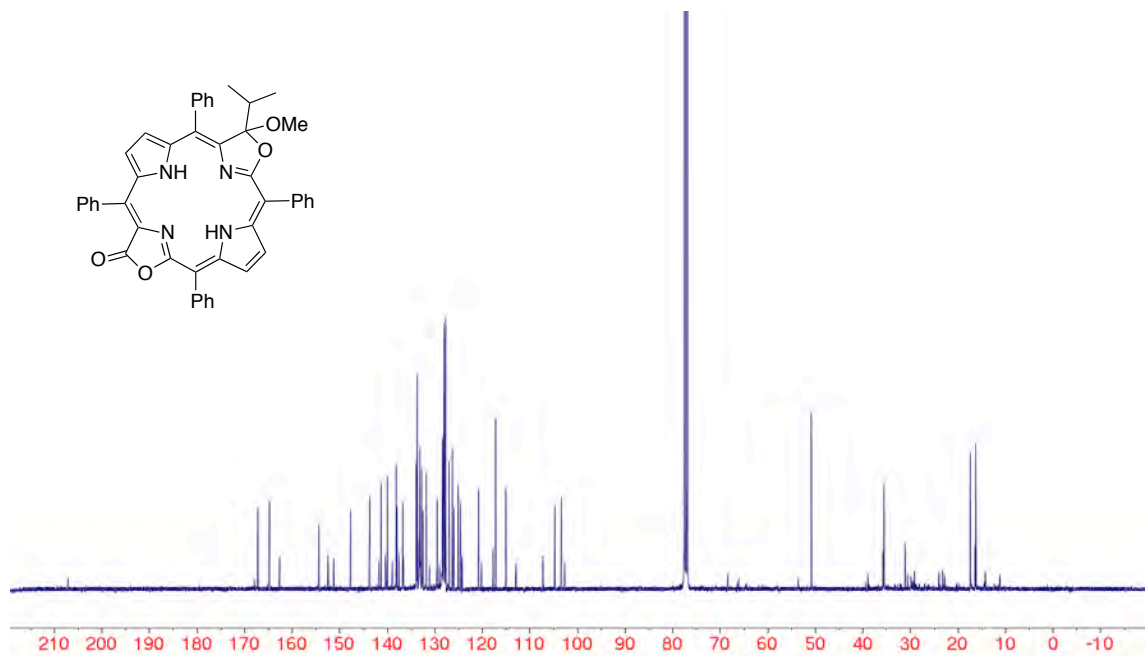


Figure 16. ^{13}C NMR spectrum (100 MHz, CDCl_3) of **16-cis**

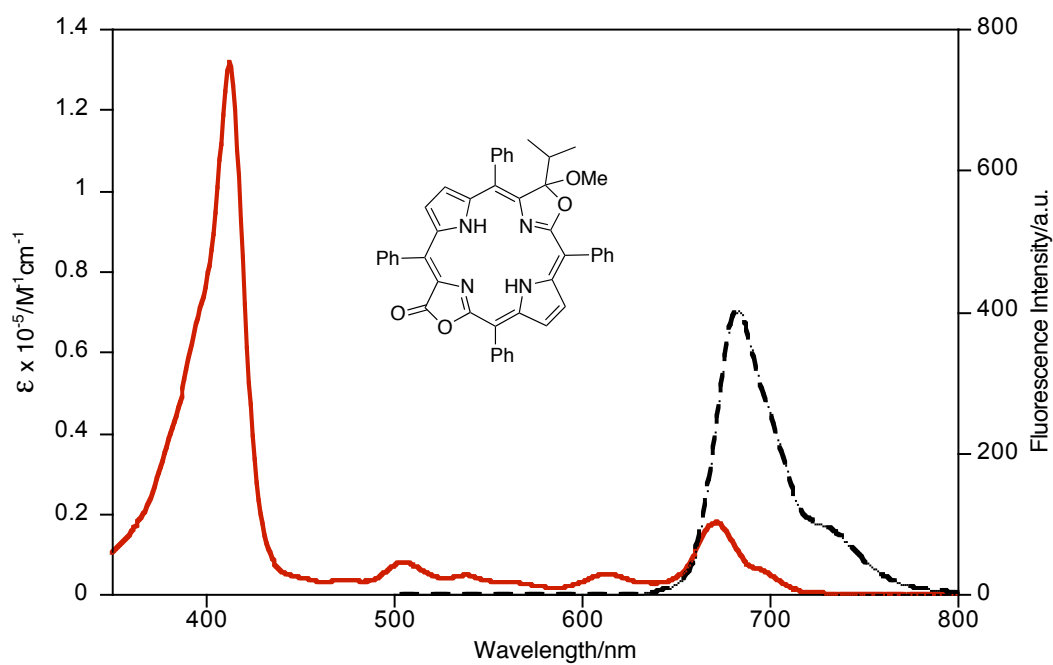


Figure 17. UV-vis (solid red trace) and fluorescence (broken black trace) spectra of **16-cis** (CH_2Cl_2)

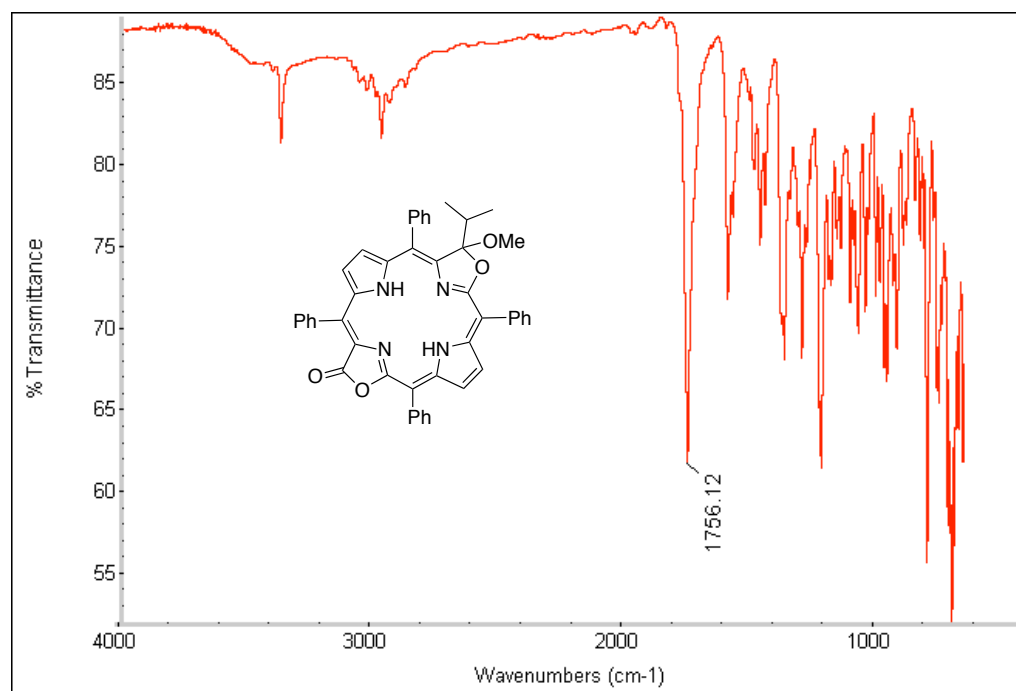
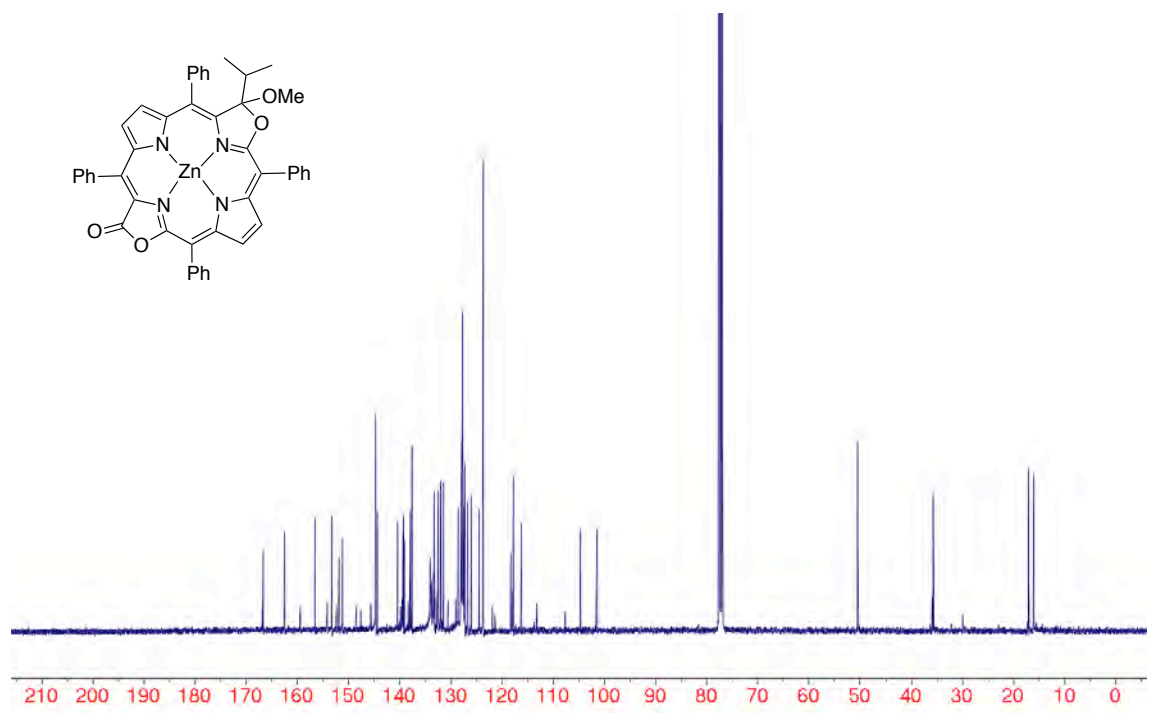
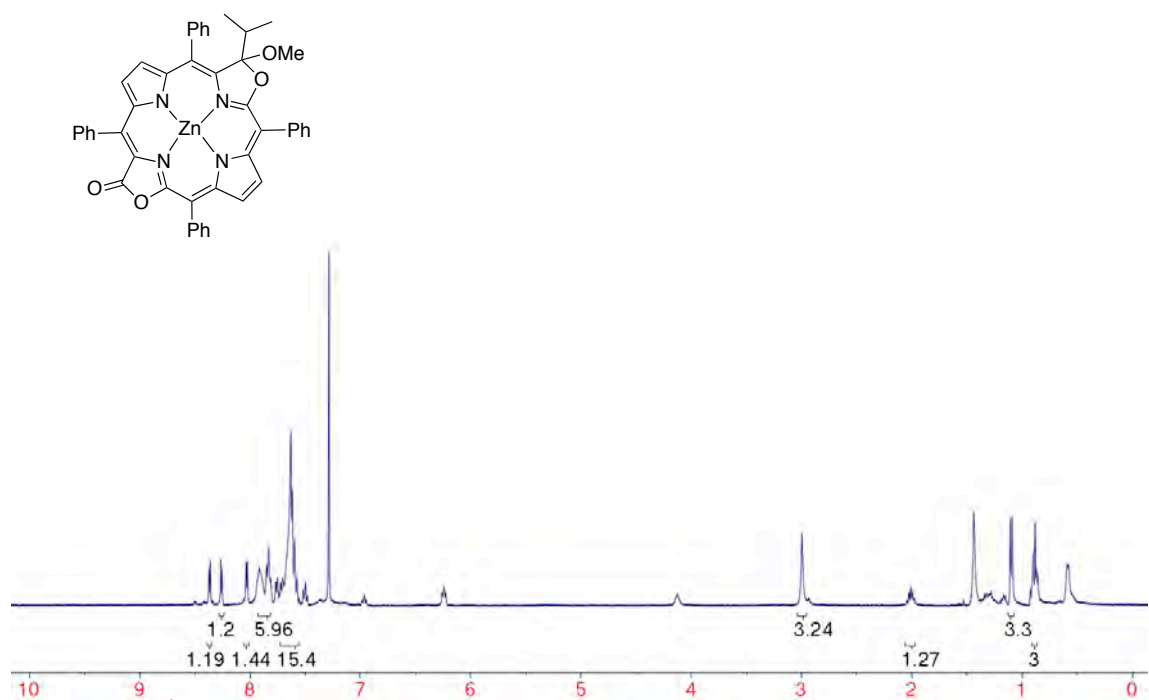


Figure 18. FT-IR spectrum (neat, diffuse reflectance) of **16-cis**



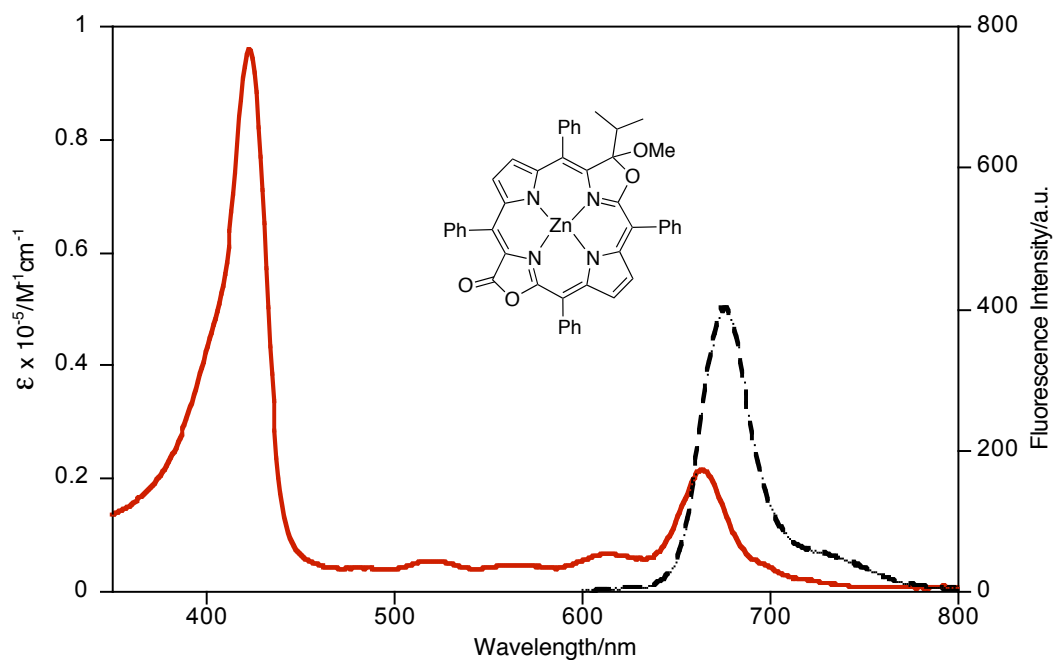


Figure 21. UV-vis (solid red trace) and fluorescence (broken black trace) spectra of **16Zn-cis** (CH_2Cl_2)

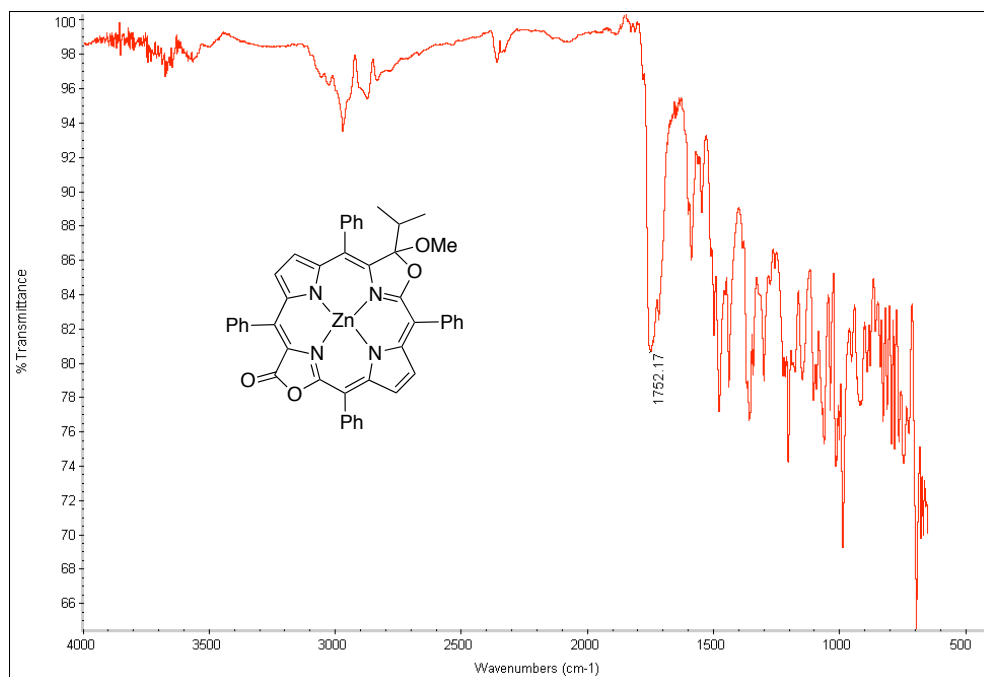


Figure 22. FT-IR spectrum (neat, diffuse reflectance) of **16Zn-cis**

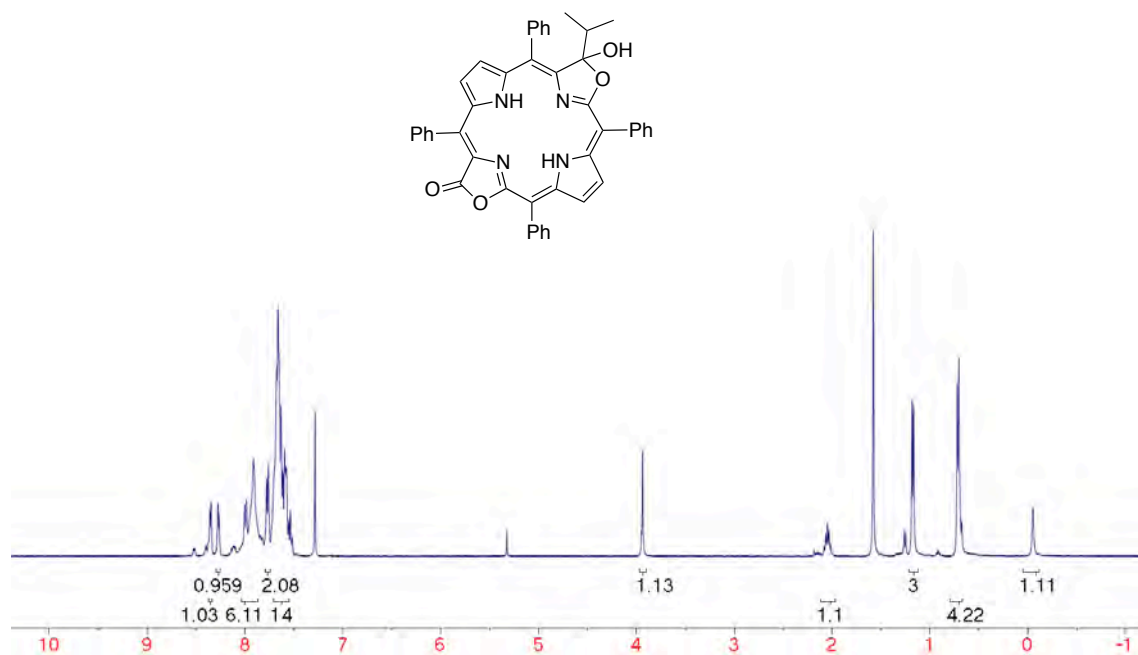


Figure 23. ^1H NMR spectrum (400 MHz, CDCl_3) of **18-cis**

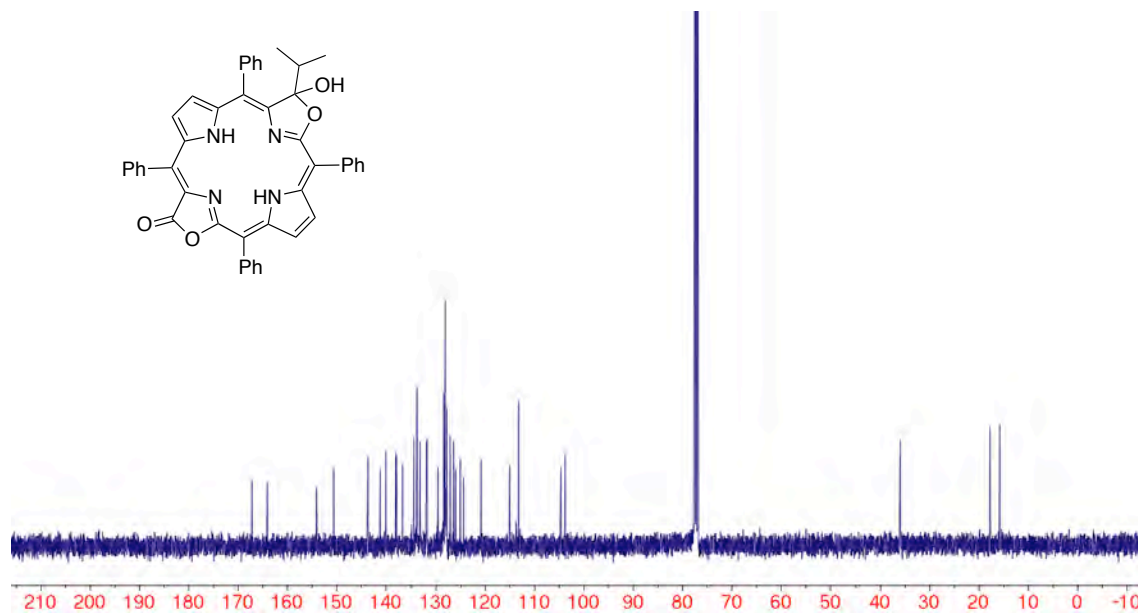


Figure 24. ^{13}C NMR spectrum (100 MHz, CDCl_3) of **18-cis**

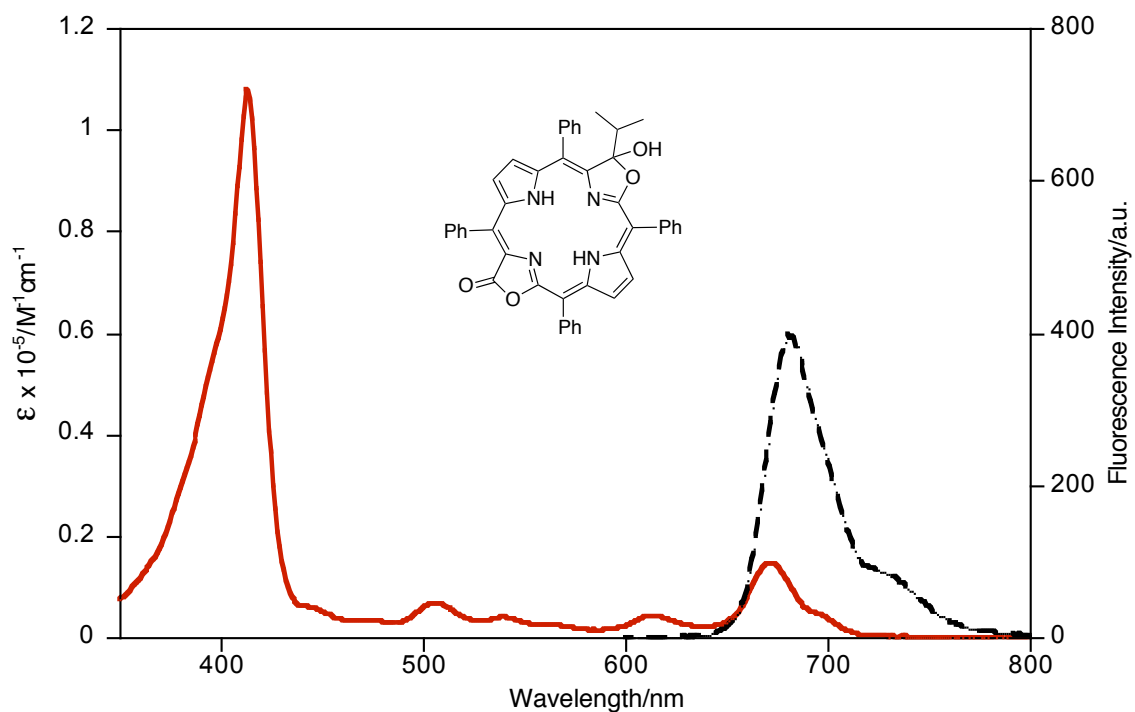


Figure 25. UV-vis (solid red trace) and fluorescence (broken black trace) spectra of **18-cis** (CH_2Cl_2)

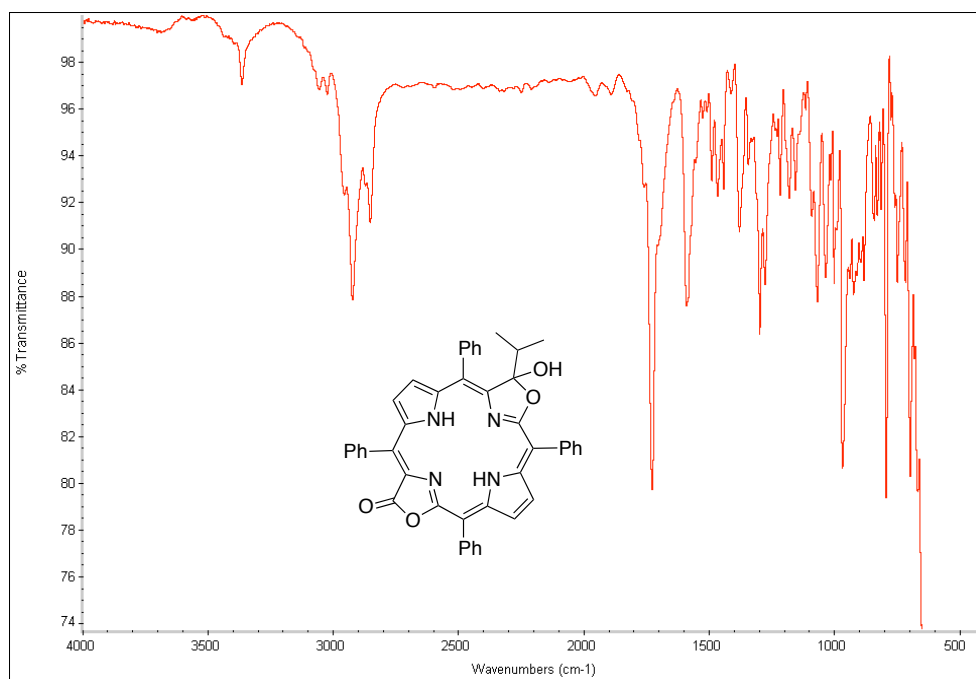


Figure 26. FT-IR spectrum (neat, diffuse reflectance) of **18-cis**

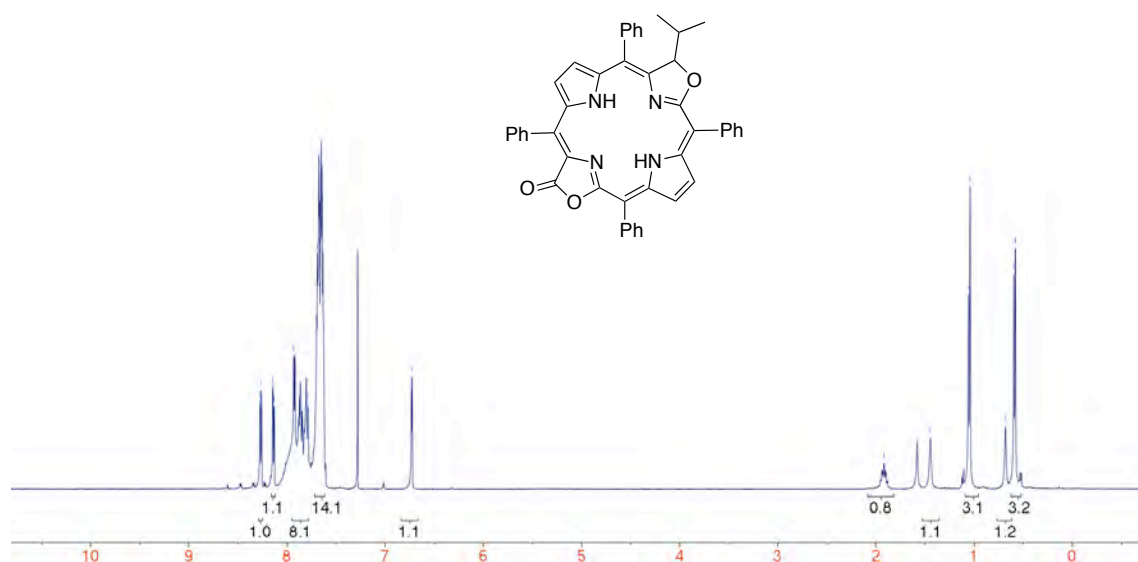


Figure 27. ^1H NMR spectrum (400 MHz, CDCl_3) of **19-cis**

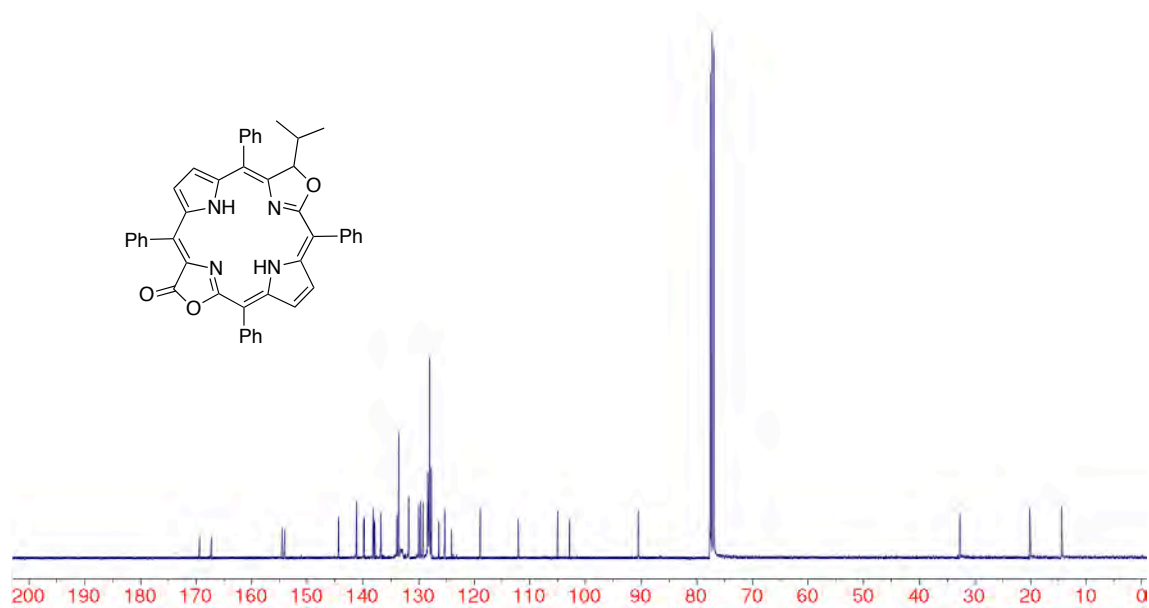


Figure 28. ^{13}C NMR spectrum (100 MHz, CDCl_3) of **19-cis**

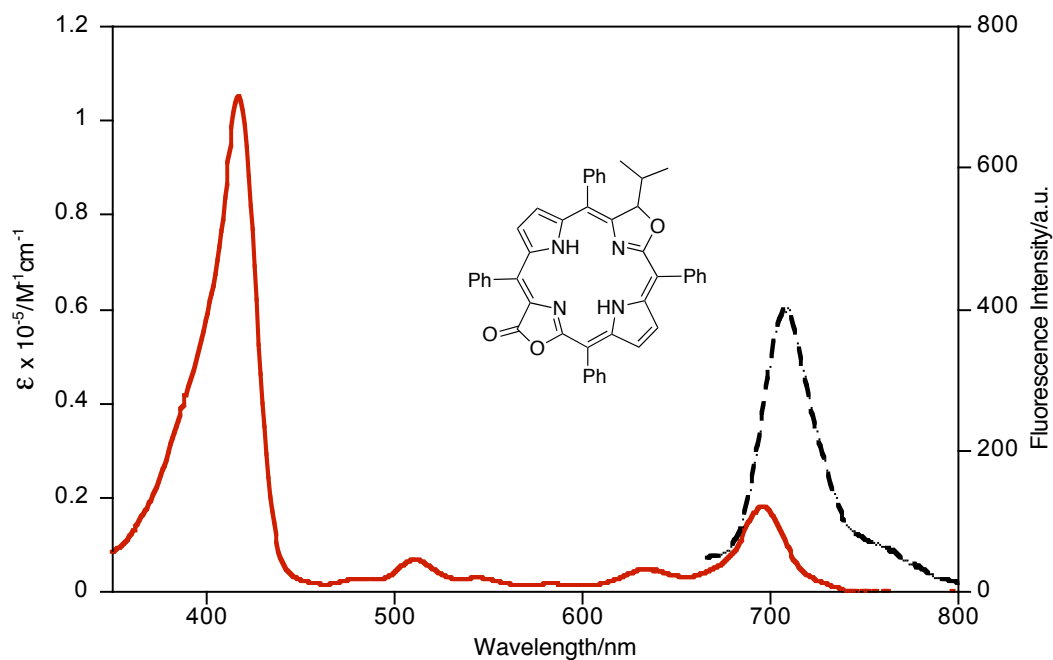


Figure 29. UV-vis (solid red trace) and fluorescence (broken black trace) spectra of **19-cis** (CH_2Cl_2)

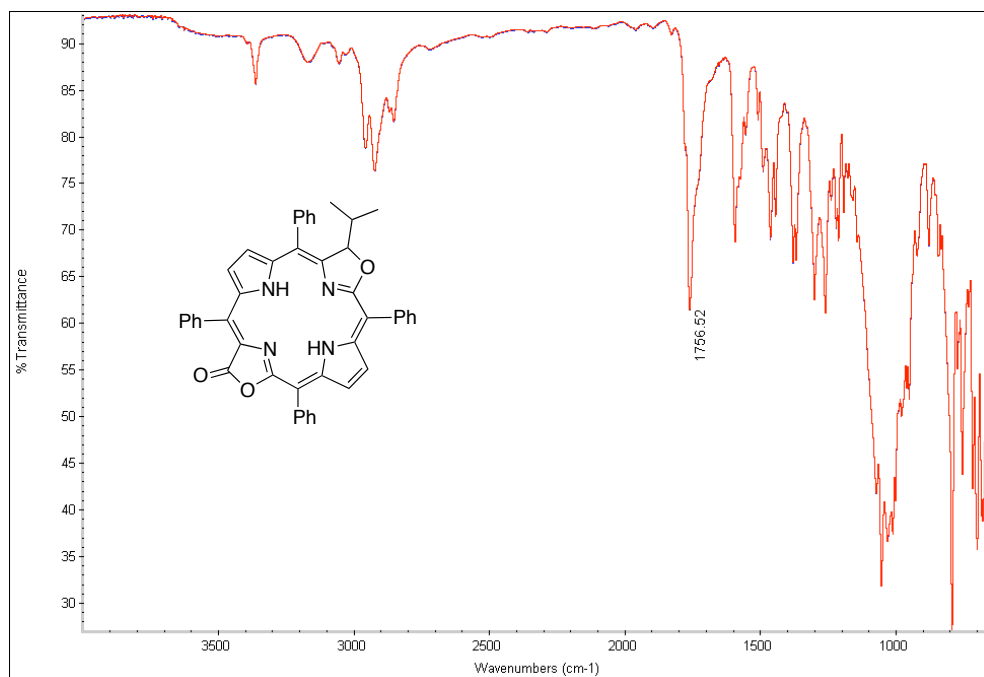
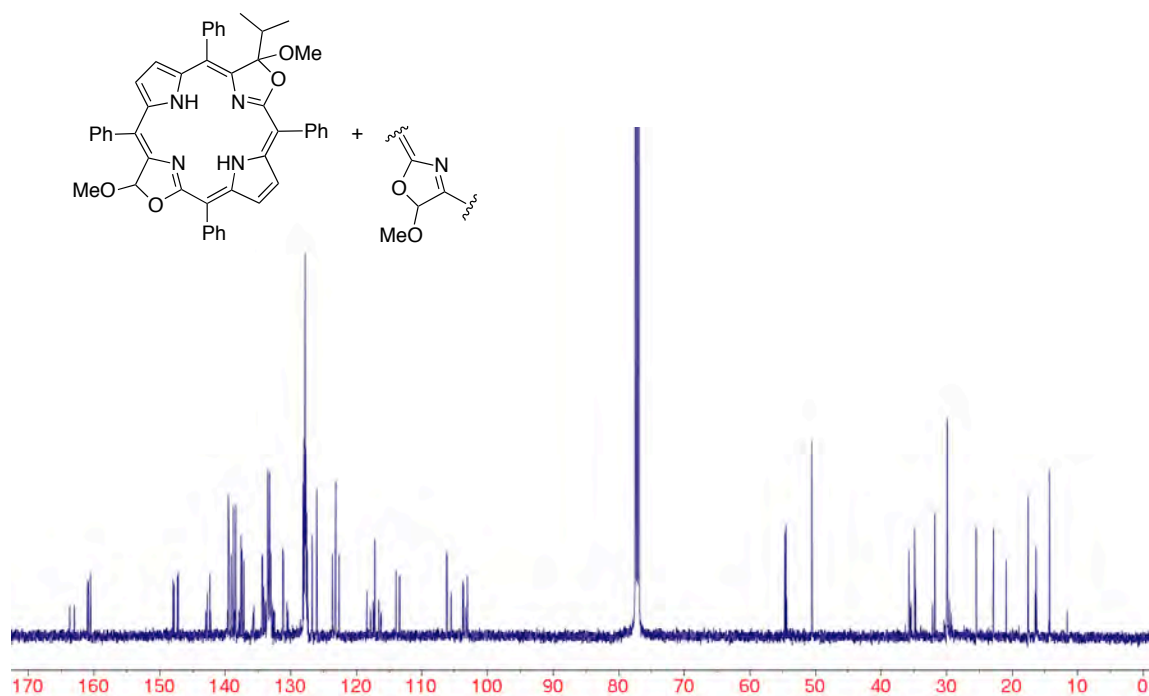
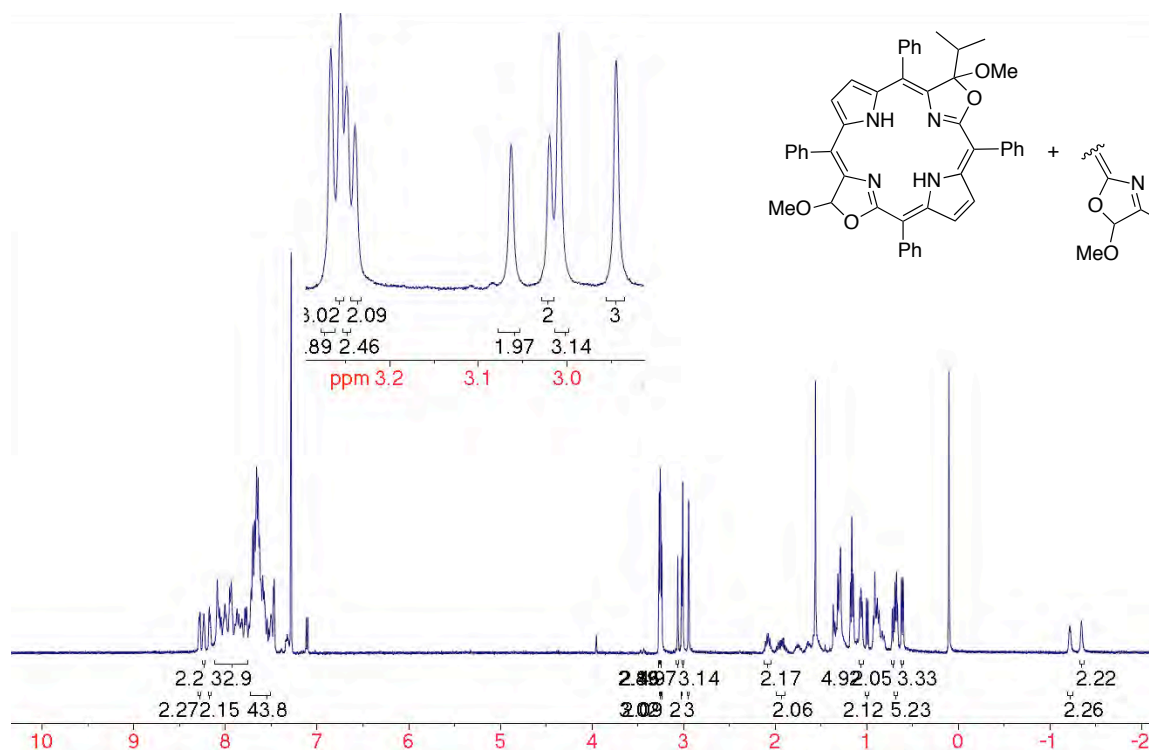


Figure 30. FT-IR spectrum (neat, diffuse reflectance) of **19-cis**



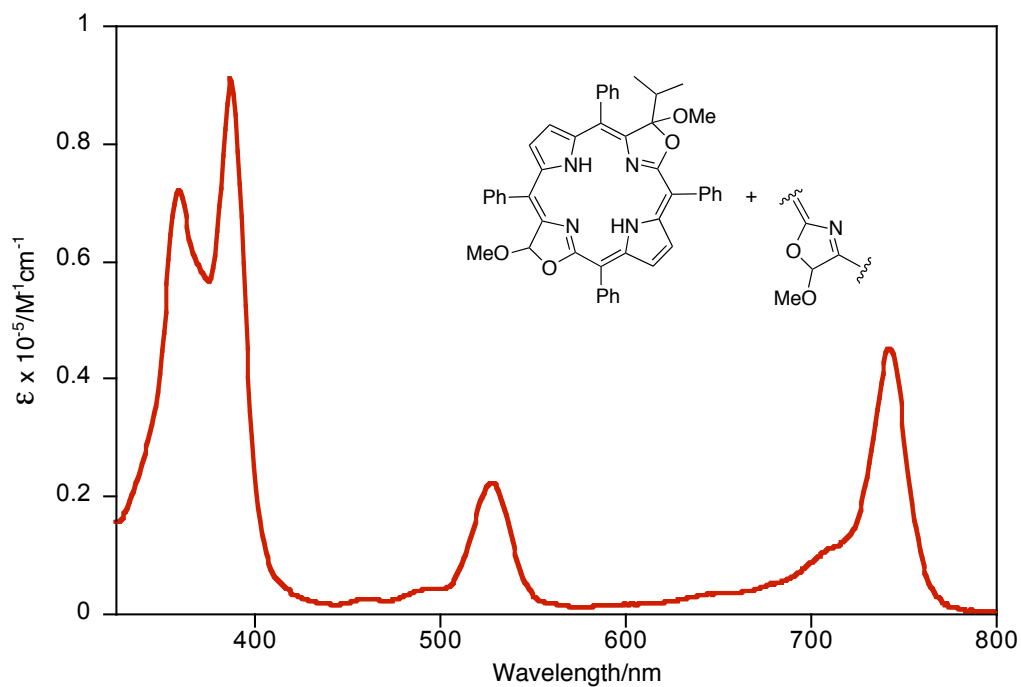


Figure 33. UV-vis spectrum of **23** (CH_2Cl_2 , mixture of all isomers)

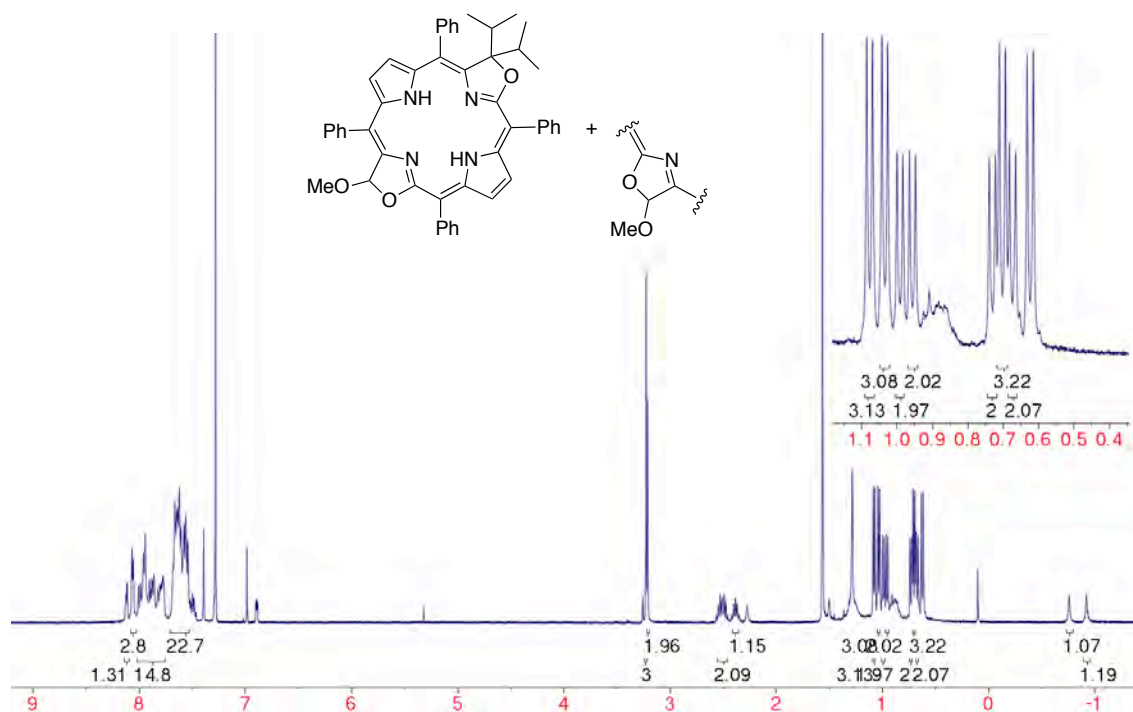


Figure 34. ^1H NMR spectrum (400 MHz, CDCl_3) of **22-cis** / **22-trans** (mixture, 3:2 favoring **22-cis**)

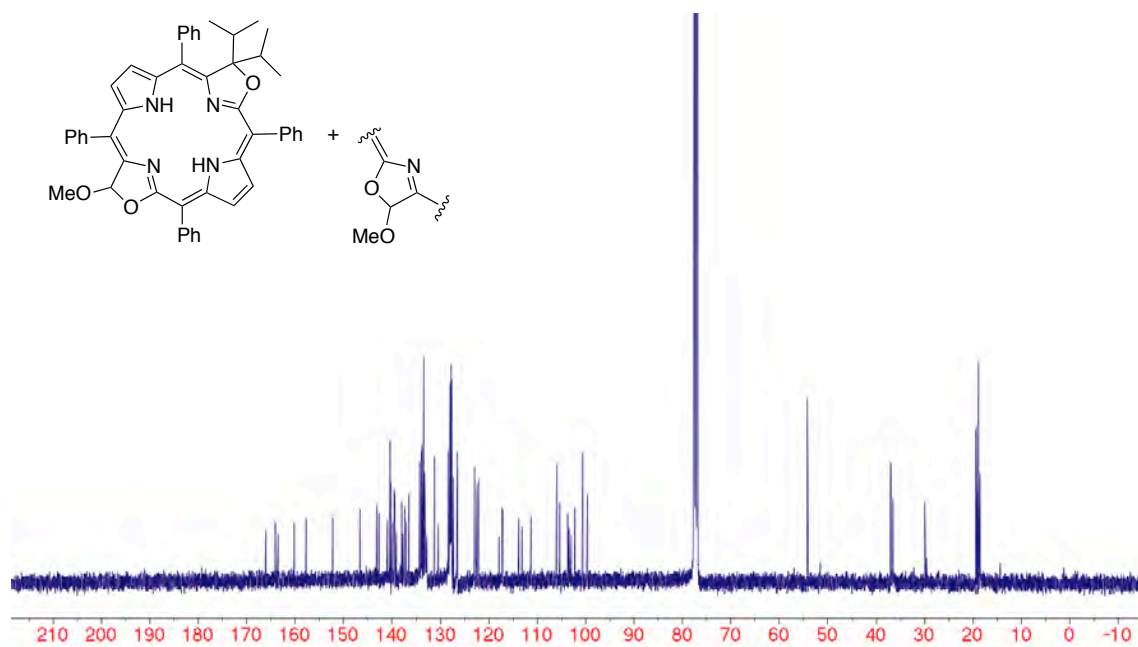


Figure 35. ^{13}C NMR spectrum (100 MHz, CDCl_3) of **22-cis** /**trans** (mixture, 3:2 favoring **22-cis**)

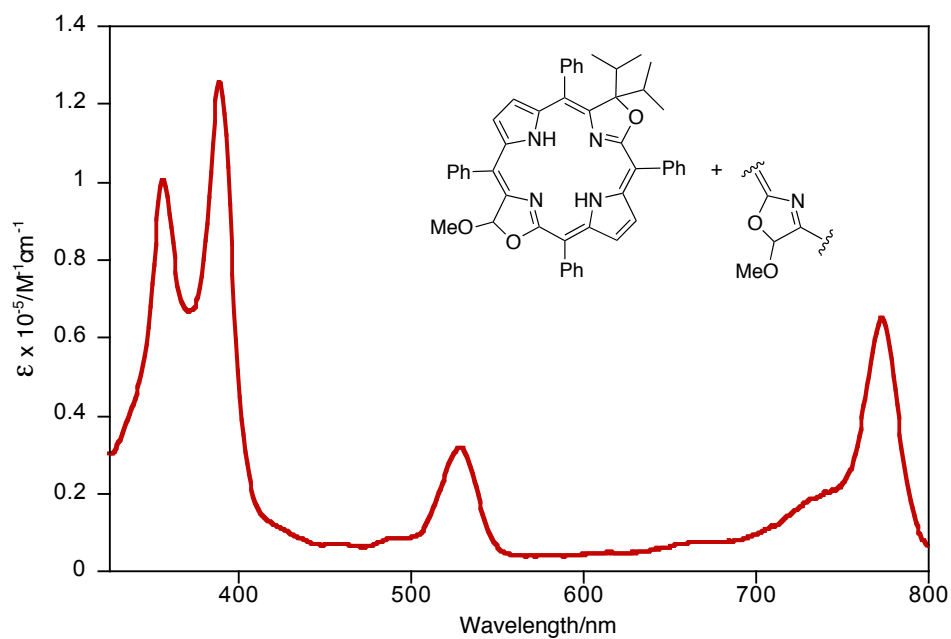
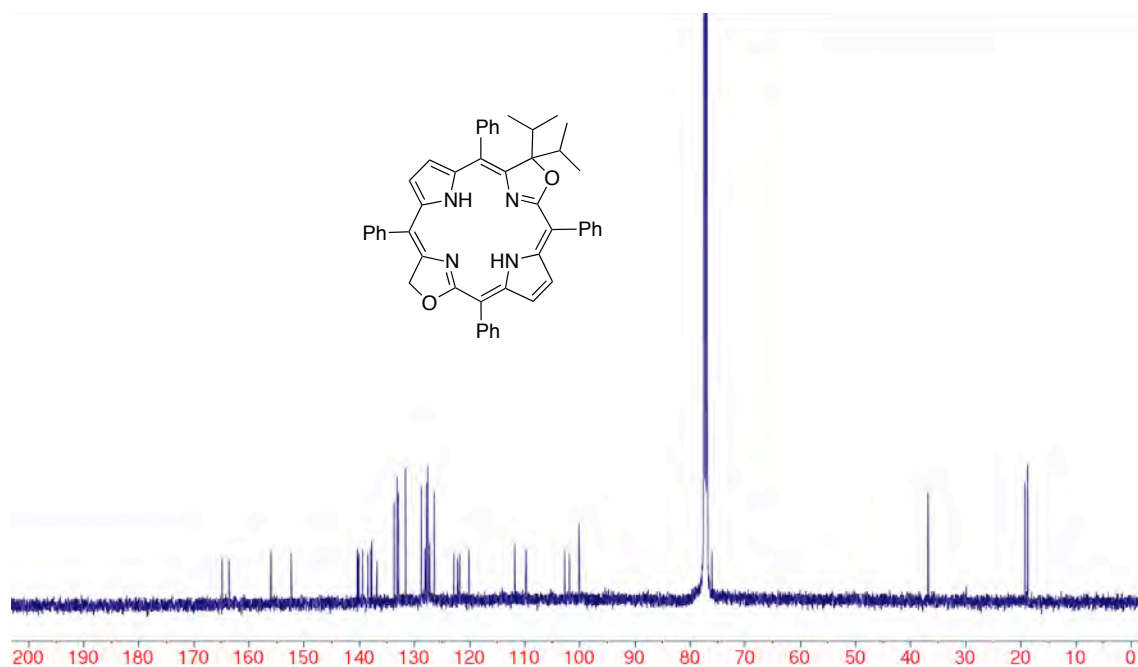
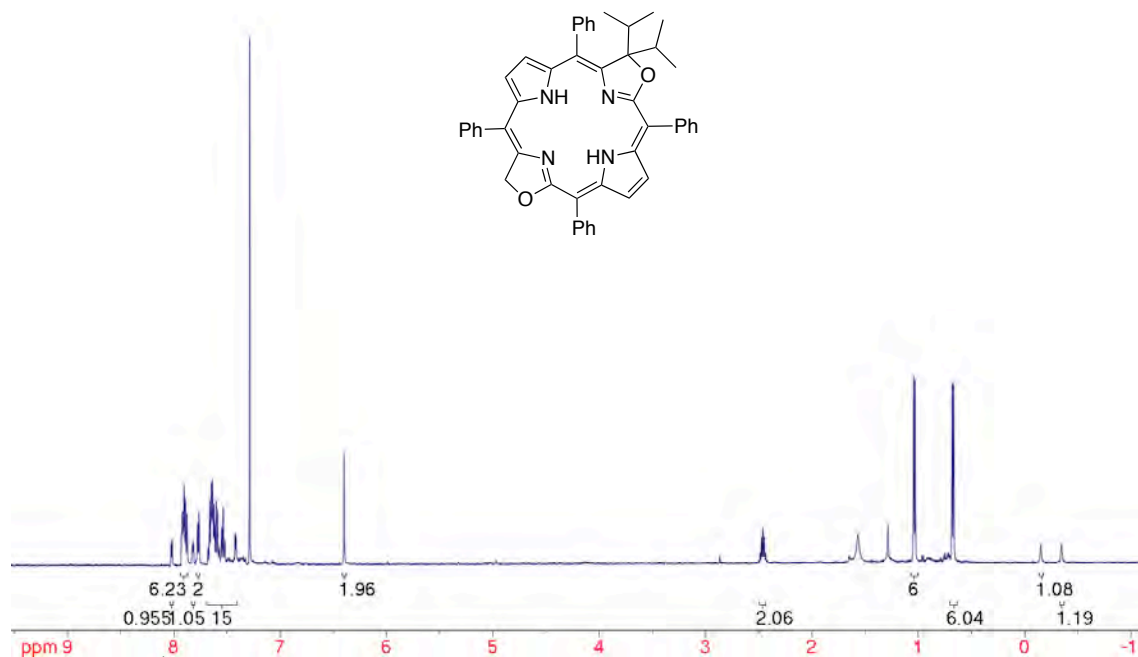


Figure 36. UV-vis spectrum of **22-cis** /**trans** (CH_2Cl_2 , mixture, 3:2 favoring **22-cis**)



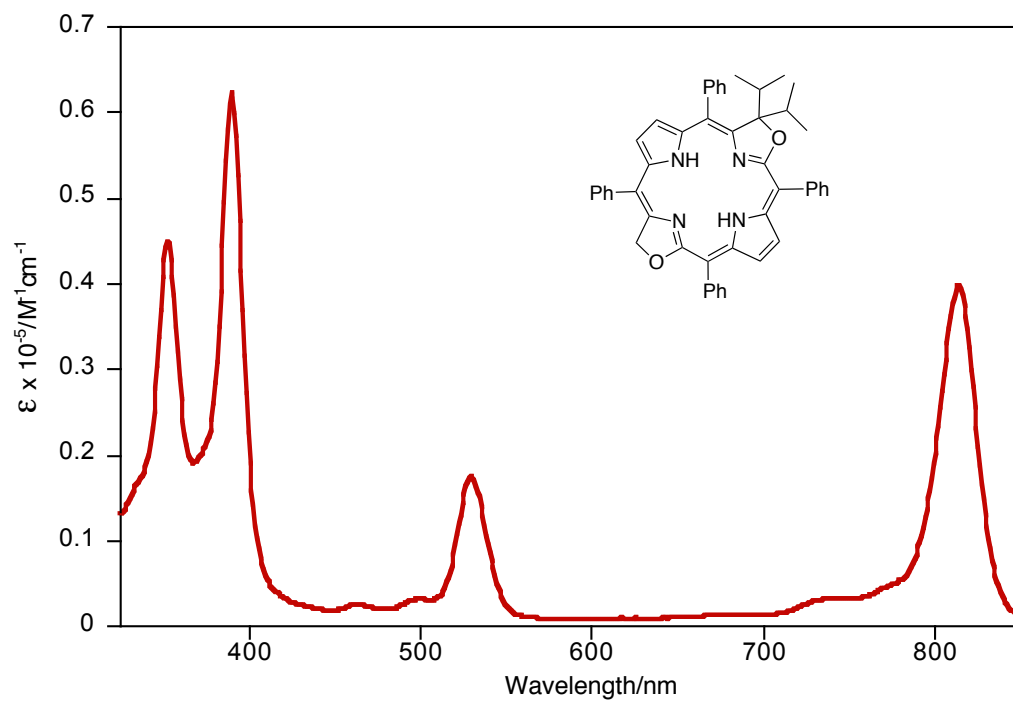


Figure 39. UV-vis spectrum of **24** (CH_2Cl_2)

Crystal Structure Report for 14-cis

A red block-like specimen of **14-cis**, approximate dimensions 0.13 mm × 0.14 mm × 0.19 mm, was used for the X-ray crystallographic analysis. The X-ray intensity data were measured. The integration of the data using a monoclinic unit cell yielded a total of 20276 reflections to a maximum θ angle of 62.99° (0.87 Å resolution), of which 5807 were independent (average redundancy 3.492, completeness = 96.5%, $R_{\text{int}} = 4.80\%$, $R_{\text{sig}} = 5.07\%$) and 4865 (83.78%) were greater than $2\sigma(F^2)$. The final cell constants of $a = 11.4410(5)$ Å, $b = 21.8550(10)$ Å, $c = 18.5306(8)$ Å, $\beta = 126.626(3)^\circ$, volume = 3718.6(3) Å³, are based upon the refinement of the XYZ-centroids of reflections above 20 $\sigma(I)$. The calculated minimum and maximum transmission coefficients (based on crystal size) are 0.8892 and 0.9220.

The structure was solved and refined using the Bruker SHELXTL Software Package, using the space group P2(1)/c, with $Z = 4$ for the formula unit, C₄₈H₄₀N₄O₃. The final anisotropic full-matrix least-squares refinement on F^2 with 573 variables converged at $R1 = 8.74\%$, for the observed data and $wR2 = 23.24\%$ for all data. The goodness-of-fit was 1.082. The largest peak in the final difference electron density synthesis was 0.328 e⁻/Å³ and the largest hole was -0.226 e⁻/Å³ with an RMS deviation of 0.053 e⁻/Å³. On the basis of the final model, the calculated density was 1.288 g/cm³ and $F(000)$, 1520 e⁻.

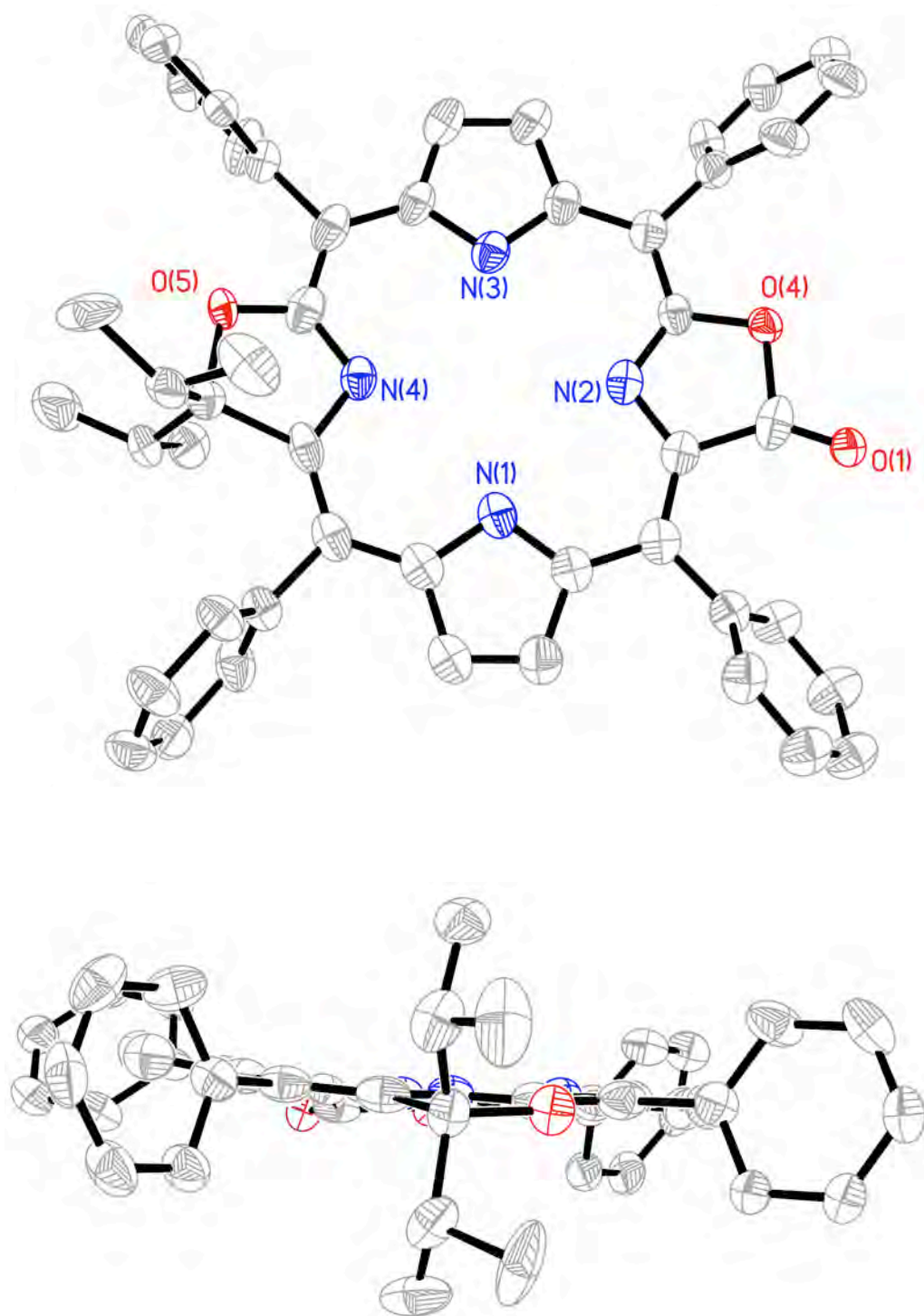


Figure 40. ORTEP Representation of the crystal structure of **14-*cis***, side and top views. Hydrogen atoms and disorder removed for clarity.

Table S1. Crystal data and structure refinement for **14-cis**.

Identification code	14-cis	
Empirical formula	$C_{48}H_{40}N_4O_3$	
Formula weight	720.84	
Temperature	100(2) K	
Wavelength	1.54178 Å	
Crystal system	Monoclinic	
Space group	P2(1)/c	
Unit cell dimensions	$a = 11.4410(5) \text{ Å}$	$\alpha = 90^\circ$
	$b = 21.8550(10) \text{ Å}$	$\beta = 126.626(3)^\circ$
	$c = 18.5306(8) \text{ Å}$	$\gamma = 90^\circ$
Volume	$3718.6(3) \text{ Å}^3$	
Z	4	
Density (calculated)	1.288 Mg/m^3	
Absorption coefficient	0.640 mm^{-1}	
F(000)	1520	
Crystal size	$0.19 \times 0.14 \times 0.13 \text{ mm}^3$	
Theta range for data collection	3.59 to 62.99° .	
Index ranges	$-13 \leq h \leq 11$, $-25 \leq k \leq 22$, $-21 \leq l \leq 20$	
Reflections collected	20276	
Independent reflections	5807 [$R(\text{int}) = 0.0480$]	
Completeness to $\theta = 62.99^\circ$	96.5 %	
Absorption correction	SADABS	
Max. and min. transmission	0.9220 and 0.8892	
Refinement method	Full-matrix least-squares on F^2	
Data / restraints / parameters	5807 / 0 / 573	
Goodness-of-fit on F^2	1.082	
Final R indices [$I > 2\sigma(I)$]	$R1 = 0.0874$, $wR2 = 0.2245$	
R indices (all data)	$R1 = 0.0987$, $wR2 = 0.2324$	
Largest diff. peak and hole	0.328 and -0.226 e.Å^{-3}	

Crystal Structure Report for 16-cis

A red plate-like specimen of **16-cis**, approximate dimensions 0.08 mm × 0.22 mm × 0.28 mm, was used for the X-ray crystallographic analysis. The X-ray intensity data were measured.

The integration of the data using a monoclinic unit cell yielded a total of 21363 reflections to a maximum θ angle of 64.61° (0.85 Å resolution), of which 6046 were independent (average redundancy 3.533, completeness = 96.4%, $R_{\text{int}} = 3.03\%$, $R_{\text{sig}} = 2.87\%$) and 5127 (84.80%) were greater than $2\sigma(F^2)$. The final cell constants of $a = 23.6921(5)$ Å, $b = 13.7480(3)$ Å, $c = 25.7494(8)$ Å, $\beta = 117.2340(10)^\circ$, volume = $7457.3(3)$ Å³, are based upon the refinement of the XYZ-centroids of reflections above $20\sigma(I)$. Data were corrected for absorption effects using the multi-scan method (SADABS). The ratio of minimum to maximum apparent transmission was 0.871. The calculated minimum and maximum transmission coefficients (based on crystal size) are 0.8320 and 0.9473.

The structure was solved and refined using the Bruker SHELXTL Software Package, using the space group $C 1 2/c 1$, with $Z = 4$ for the formula unit, $C_{97}H_{77}N_9O_8$. The final anisotropic full-matrix least-squares refinement on F^2 with 518 variables converged at $R1 = 5.16\%$, for the observed data and $wR2 = 15.51\%$ for all data. The goodness-of-fit was 0.967. The largest peak in the final difference electron density synthesis was $0.797\text{ e}^-/\text{\AA}^3$ and the largest hole was $-0.386\text{ e}^-/\text{\AA}^3$ with an RMS deviation of $0.056\text{ e}^-/\text{\AA}^3$. On the basis of the final model, the calculated density was 1.333 g/cm^3 and $F(000)$, 3144 e^- .

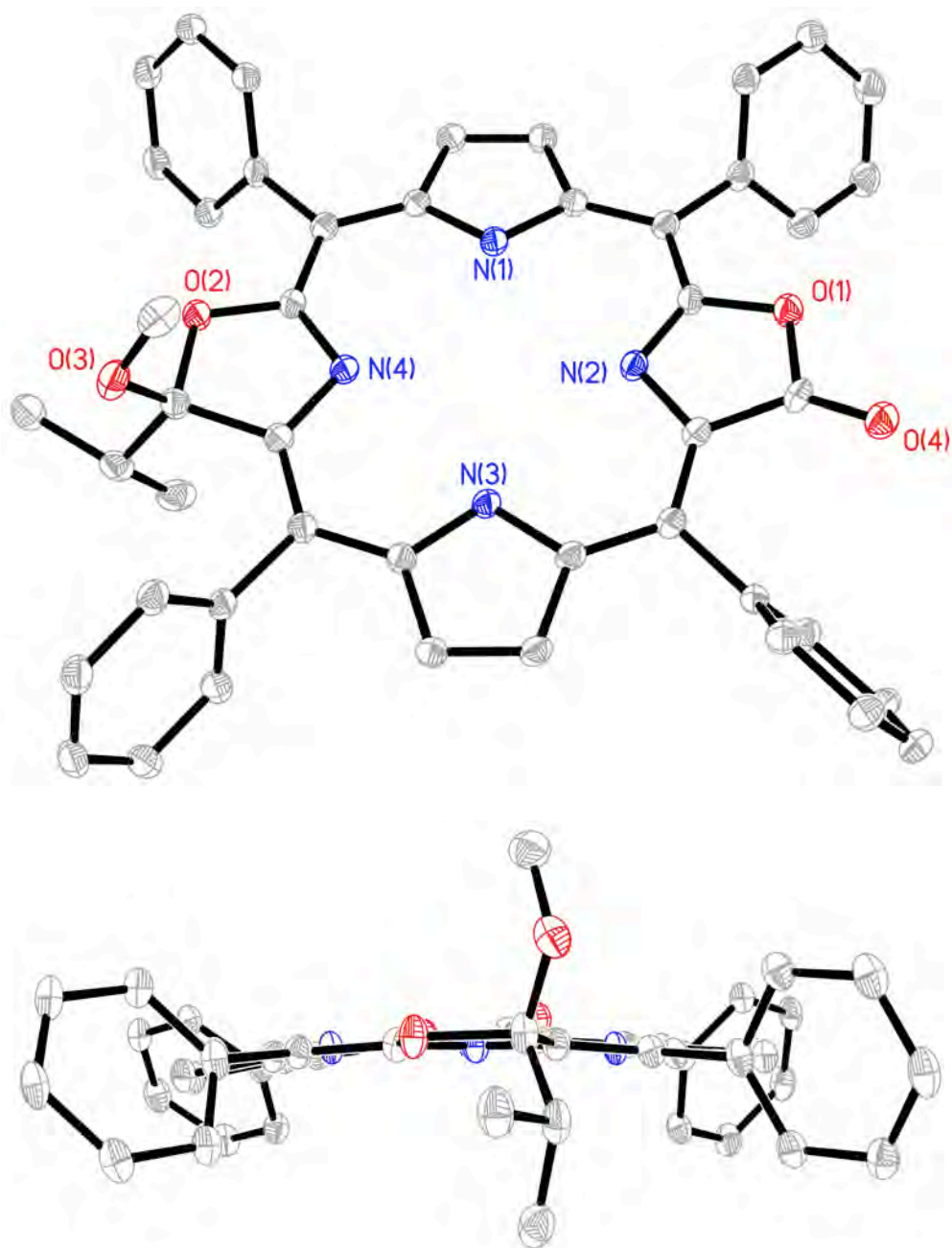


Figure 41. ORTEP Representation of the crystal structure of **16-cis**, side and top views. Hydrogen atoms and disorder removed for clarity.

Table S2. Crystal data and structure refinement for **16-cis**.

Identification code	16-cis
Empirical formula	C ₉₇ H ₇₇ N ₉ O ₈
Formula weight	1496.68
Temperature	100(2) K
Wavelength	1.54178 Å
Crystal system	Monoclinic
Space group	C2/c
Unit cell dimensions	a = 23.6921(5) Å α = 90° b = 13.7480(3) Å β = 117.2340(10)° c = 25.7494(8) Å γ = 90°
Volume	7457.3(3) Å ³
Z	4
Density (calculated)	1.333 Mg/m ³
Absorption coefficient	0.684 mm ⁻¹
F(000)	3144
Crystal size	0.28 × 0.22 × 0.08 mm ³
Theta range for data collection	3.84 to 64.61°.
Index ranges	-27 ≤ h ≤ 26, -16 ≤ k ≤ 16, -30 ≤ l ≤ 29
Reflections collected	21363
Independent reflections	6046 [R(int) = 0.0303]
Completeness to theta = 64.61°	96.4 %
Absorption correction	SADABS
Max. and min. transmission	0.9473 and 0.8320
Refinement method	Full-matrix least-squares on F ²
Data / restraints / parameters	6046 / 0 / 518
Goodness-of-fit on F ²	0.967
Final R indices [I > 2σ(I)]	R1 = 0.0516, wR2 = 0.1466
R indices (all data)	R1 = 0.0607, wR2 = 0.1551
Largest diff. peak and hole	0.797 and -0.386 e.Å ⁻³

Crystal Structure Report for 16Zn-cis

A green specimen of **16Zn-cis**, approximate dimensions 0.27 mm × 0.47 mm × 0.55 mm, was used for the X-ray crystallographic analysis. The X-ray intensity data were measured.

The integration of the data using a triclinic unit cell yielded a total of 23334 reflections to a maximum θ angle of 61.00° (0.88 Å resolution), of which 6348 were independent (average redundancy 3.676, completeness = 94.7%, $R_{\text{int}} = 2.72\%$, $R_{\text{sig}} = 2.19\%$) and 6109 (96.24%) were greater than $2\sigma(F^2)$. The final cell constants of $a = 12.5921(4)$ Å, $b = 12.9701(4)$ Å, $c = 14.8500(5)$ Å, $\alpha = 111.9920(10)^\circ$, $\beta = 96.5610(10)^\circ$, $\gamma = 97.7270(10)^\circ$, volume = $2192.37(12)$ Å³, are based upon the refinement of the XYZ-centroids of reflections above $20\sigma(I)$. The calculated minimum and maximum transmission coefficients (based on crystal size) are 0.5661 and 0.7434.

The structure was solved and refined using the Bruker SHELXTL Software Package, using the space group P -1, with $Z = 2$ for the formula unit, $\text{C}_{47}\text{H}_{38}\text{N}_4\text{O}_5\text{Zn}$. The final anisotropic full-matrix least-squares refinement on F^2 with 522 variables converged at $R1 = 6.29\%$, for the observed data and $wR2 = 17.48\%$ for all data. The goodness-of-fit was 0.968. The largest peak in the final difference electron density synthesis was $1.736\text{ e}^-/\text{\AA}^3$ and the largest hole was $-0.441\text{ e}^-/\text{\AA}^3$ with an RMS deviation of $0.080\text{ e}^-/\text{\AA}^3$. On the basis of the final model, the calculated density was 1.218 g/cm^3 and $F(000)$, 836 e^- .

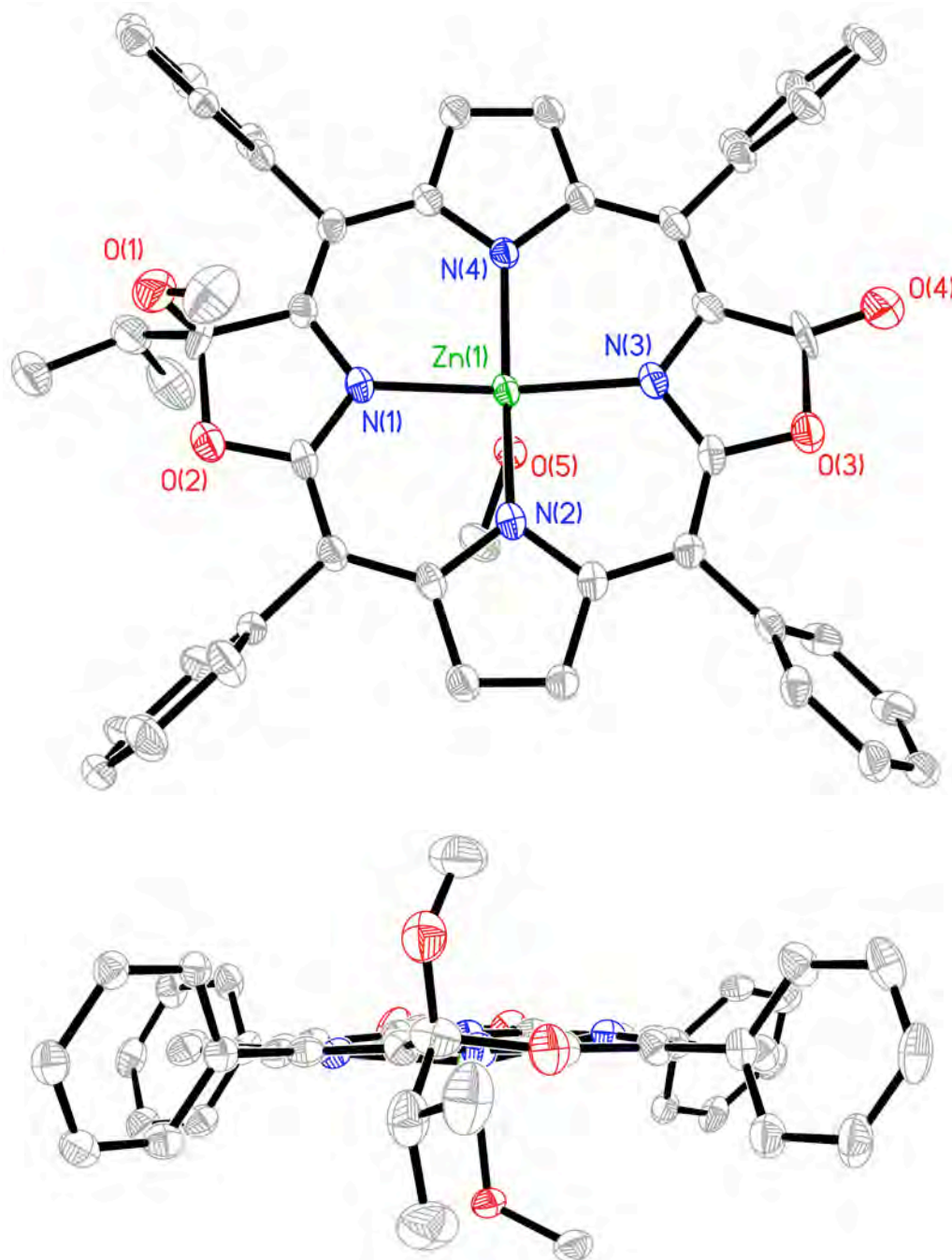


Figure 42. ORTEP Representation of the crystal structure of **16Zn-cis**, side and top views. Hydrogen atoms and disorder removed for clarity.

Table S3. Crystal data and structure refinement for **16Zn-cis**.

Identification code	16Zn-cis	
Empirical formula	C ₄₇ H ₃₈ N ₄ O ₅ Zn	
Formula weight	804.18	
Temperature	100(2) K	
Wavelength	1.54178 Å	
Crystal system	Triclinic	
Space group	P1	
Unit cell dimensions	a = 12.5921(4) Å	α = 111.9920(10)°
	b = 12.9701(4) Å	β = 96.5610(10)°
	c = 14.8500(5) Å	γ = 97.7270(10)°
Volume	2192.36(12) Å ³	
Z	2	
Density (calculated)	1.218 Mg/m ³	
Absorption coefficient	1.163 mm ⁻¹	
F(000)	836	
Crystal size	0.55 × 0.47 × 0.27 mm	
Theta range for data collection	3.26 to 61.00°.	
Index ranges	-14 ≤ h ≤ 14, -14 ≤ k ≤ 11, -16 ≤ l ≤ 16	
Reflections collected	23334	
Independent reflections	6348 [R(int) = 0.0272]	
Completeness to theta = 61.00°	94.7 %	
Absorption correction	SADABS	
Max. and min. transmission	0.7434 and 0.5661	
Refinement method	Full-matrix least-squares on F ²	
Data / restraints / parameters	6348 / 0 / 522	
Goodness-of-fit on F ²	0.968	
Final R indices [I > 2σ(I)]	R1 = 0.0629, wR2 = 0.1734	
R indices (all data)	R1 = 0.0645, wR2 = 0.1748	
Largest diff. peak and hole	1.736 and -0.441 e.Å ⁻³	

Crystal Structure Report for **23-trans-E**

An orange plate-like specimen of **23-trans-E**, approximate dimensions 0.09 mm × 0.10 mm × 0.21 mm, was used for the X-ray crystallographic analysis. The X-ray intensity data were measured.

The total exposure time was 33.52 hours. The frames were integrated with the Bruker SAINT software package using a narrow-frame algorithm. The integration of the data using an orthorhombic unit cell yielded a total of 42976 reflections to a maximum θ angle of 63.00° (0.87 Å resolution), of which 6168 were independent (average redundancy 6.968, completeness = 100.0%, $R_{\text{int}} = 7.20\%$, $R_{\text{sig}} = 4.31\%$) and 5590 (90.63%) were greater than $2\sigma(F^2)$. The final cell constants of $a = 9.4468(2)$ Å, $b = 13.2846(3)$ Å, $c = 30.4999(7)$ Å, volume = 3827.64(15) Å³, are based upon the refinement of the XYZ-centroids of 9852 reflections above $20\sigma(I)$ with $5.795^\circ < 2\theta < 123.8^\circ$. Data were corrected for absorption effects using the multi-scan method (SADABS). The ratio of minimum to maximum apparent transmission was 0.854. The calculated minimum and maximum transmission coefficients (based on crystal size) are 0.8772 and 0.9438.

The structure was solved and refined using the Bruker SHELXTL Software Package, using the space group P2(1)2(1)2(1), with $Z = 4$ for the formula unit, C₄₇H₄₀N₄O₄. The final anisotropic full-matrix least-squares refinement on F² with 519 variables converged at $R1 = 8.08\%$, for the observed data and $wR2 = 22.13\%$ for all data. The goodness-of-fit was 0.945. The largest peak in the final difference electron density synthesis was 1.354 e⁻/Å³ and the largest hole was -0.389 e⁻/Å³ with an RMS deviation of 0.073 e⁻/Å³. On the basis of the final model, the calculated density was 1.258 g/cm³ and F(000), 1528 e⁻.

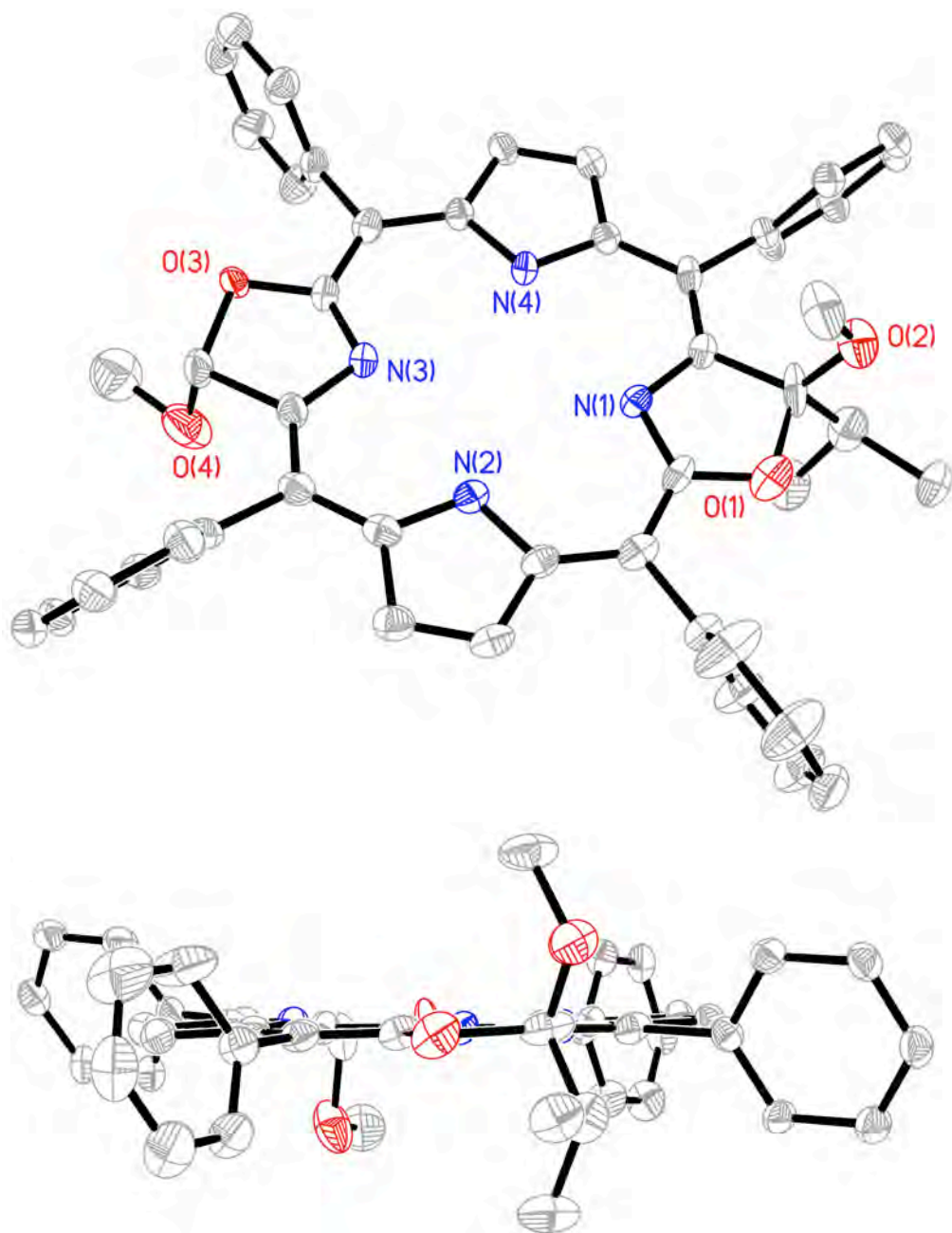


Figure 43. ORTEP Representation of the crystal structure of **23-trans-E**, side and top views. Hydrogen atoms and disorder removed for clarity.

Table S4. Crystal data and structure refinement for **23-trans-E**

Identification code	23-trans-E	
Empirical formula	C ₄₇ H ₄₀ N ₄ O ₄	
Formula weight	724.83	
Temperature	100(2) K	
Wavelength	1.54178 Å	
Crystal system	Orthorhombic	
Space group	P2(1)2(1)2(1)	
Unit cell dimensions	a = 9.4468(2) Å	α = 90°
	b = 13.2846(3) Å	β = 90°
	c = 30.4999(7) Å	γ = 90°
Volume	3827.64(15) Å ³	
Z	4	
Density (calculated)	1.258 Mg/m ³	
Absorption coefficient	0.644 mm ⁻¹	
F(000)	1528	
Crystal size	0.21 × 0.10 × 0.09 mm ³	
Theta range for data collection	2.90 to 63.00°.	
Index ranges	-9 ≤ h ≤ 10, -15 ≤ k ≤ 15, -35 ≤ l ≤ 35	
Reflections collected	42976	
Independent reflections	6168 [R(int) = 0.0720]	
Completeness to theta = 63.00°	100.0 %	
Absorption correction	SADABS	
Max. and min. transmission	0.9437 and 0.8772	
Refinement method	Full-matrix least-squares on F ²	
Data / restraints / parameters	6168 / 24 / 519	
Goodness-of-fit on F ²	0.945	
Final R indices [I > 2σ(I)]	R1 = 0.0808, wR2 = 0.2144	
R indices (all data)	R1 = 0.0876, wR2 = 0.2213	
Absolute structure parameter	0.9(6)	
Largest diff. peak and hole	1.354 and -0.389 e.Å ⁻³	

Crystal Structure Report for **23-trans-Z**

A orange specimen of **23-trans-Z**, approximate dimensions 0.18 mm × 0.24 mm × 0.28 mm, was used for the X-ray crystallographic analysis. The X-ray intensity data were measured.

The total exposure time was 38.48 hours. The frames were integrated with the Bruker SAINT software package using a narrow-frame algorithm. The integration of the data using a monoclinic unit cell yielded a total of 37579 reflections to a maximum θ angle of 61.98° (0.87 Å resolution), of which 5901 were independent (average redundancy 6.368, completeness = 99.8%, $R_{\text{int}} = 4.98\%$, $R_{\text{sig}} = 3.56\%$) and 4716 (79.92%) were greater than $2\sigma(F^2)$. The final cell constants of $a = 20.5804(4)$ Å, $b = 9.5370(2)$ Å, $c = 19.1964(4)$ Å, $\beta = 91.8000(10)^\circ$, volume = $3765.92(13)$ Å³, are based upon the refinement of the XYZ-centroids of 164 reflections above $20\sigma(I)$ with $17.70^\circ < 2\theta < 97.69^\circ$. Data were corrected for absorption effects using the multi-scan method (SADABS). The ratio of minimum to maximum apparent transmission was 0.824. The calculated minimum and maximum transmission coefficients (based on crystal size) are 0.8401 and 0.8891.

The structure was solved and refined using the Bruker SHELXTL Software Package, using the space group P 2(1)/c, with $Z = 4$ for the formula unit, C₄₇H₄₀N₄O₄. The final anisotropic full-matrix least-squares refinement on F^2 with 519 variables converged at $R_1 = 8.14\%$, for the observed data and $wR_2 = 25.49\%$ for all data. The goodness-of-fit was 0.894. The largest peak in the final difference electron density synthesis was $1.444\text{ e}^-/\text{\AA}^3$ and the largest hole was $-0.439\text{ e}^-/\text{\AA}^3$ with an RMS deviation of $0.064\text{ e}^-/\text{\AA}^3$. On the basis of the final model, the calculated density was 1.278 g/cm^3 and $F(000)$, 1528 e⁻.

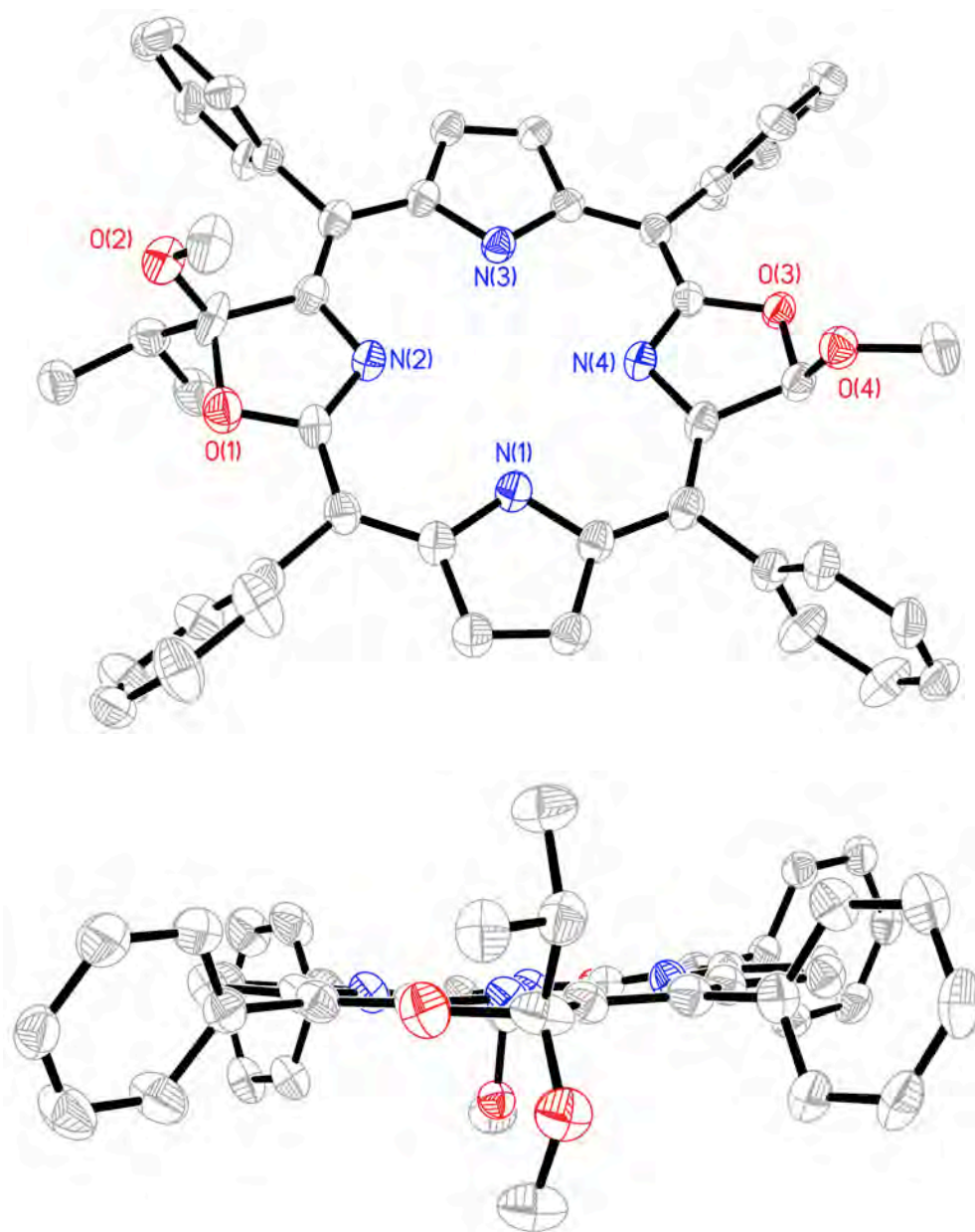


Figure 44. ORTEP Representation of the crystal structure of **23-*trans*-Z**, side and top views. Hydrogen atoms and disorder removed for clarity.

Table S5. Crystal data and structure refinement for **23-trans-Z**

Identification code	23-trans-Z	
Empirical formula	$C_{47}H_{40}N_4O_4$	
Formula weight	724.83	
Temperature	100(2) K	
Wavelength	1.54178 Å	
Crystal system	Monoclinic	
Space group	P2(1)/c	
Unit cell dimensions	$a = 20.5804(4)$ Å	$\alpha = 90^\circ$
	$b = 9.5370(2)$ Å	$\beta = 91.80(10)^\circ$
	$c = 19.1964(4)$ Å	$\gamma = 90^\circ$
Volume	3765.92(13) Å ³	
Z	4	
Density (calculated)	1.278 Mg/m ³	
Absorption coefficient	0.654 mm ⁻¹	
F(000)	1528	
Crystal size	0.28 × 0.24 × 0.18 mm ³	
Theta range for data collection	4.30 to 61.98°.	
Index ranges	-23 ≤ h ≤ 23, -10 ≤ k ≤ 10, -21 ≤ l ≤ 20	
Reflections collected	37579	
Independent reflections	5901 [R(int) = 0.0498]	
Completeness to theta = 61.98°	99.8 %	
Absorption correction	None	
Max. and min. transmission	0.8891 and 0.8401	
Refinement method	Full-matrix least-squares on F ²	
Data / restraints / parameters	5901 / 0 / 519	
Goodness-of-fit on F ²	0.894	
Final R indices [I > 2σ(I)]	R1 = 0.0814, wR2 = 0.2308	
R indices (all data)	R1 = 0.0970, wR2 = 0.2549	
Largest diff. peak and hole	1.444 and -0.439 e.Å ⁻³	

Crystal Structure Report for **22-cis**

A red specimen of **22-cis**, approximate dimensions 0.38 mm × 0.42 mm × 0.55 mm, was used for the X-ray crystallographic analysis. The X-ray intensity data were measured.

The integration of the data using a monoclinic unit cell yielded a total of 23323 reflections to a maximum θ angle of 64.45° (0.85 Å resolution), of which 6350 were independent (average redundancy 3.673, completeness = 96.1%, $R_{\text{int}} = 3.15\%$, $R_{\text{sig}} = 2.24\%$) and 5451 (85.84%) were greater than $2\sigma(F^2)$. The final cell constants of $a = 20.3320(5)$ Å, $b = 11.1841(3)$ Å, $c = 18.4019(5)$ Å, $\beta = 109.5870(10)^\circ$, volume = $3942.36(18)$ Å³, are based upon the refinement of the XYZ-centroids of reflections above $20\sigma(I)$. The calculated minimum and maximum transmission coefficients (based on crystal size) are 0.7297 and 0.8006.

The structure was solved and refined using the Bruker SHELXTL Software Package, using the space group $P2(1)/c$, with $Z = 4$ for the formula unit, $C_{49}H_{44}N_4O_3$. The final anisotropic full-matrix least-squares refinement on F^2 with 585 variables converged at $R1 = 8.25\%$, for the observed data and $wR2 = 26.74\%$ for all data. The goodness-of-fit was 1.037. The largest peak in the final difference electron density synthesis was $1.341 \text{ e}^-/\text{\AA}^3$ and the largest hole was $-0.423 \text{ e}^-/\text{\AA}^3$ with an RMS deviation of $0.056 \text{ e}^-/\text{\AA}^3$. On the basis of the final model, the calculated density was 1.242 g/cm^3 and $F(000)$, 1560 e^- .

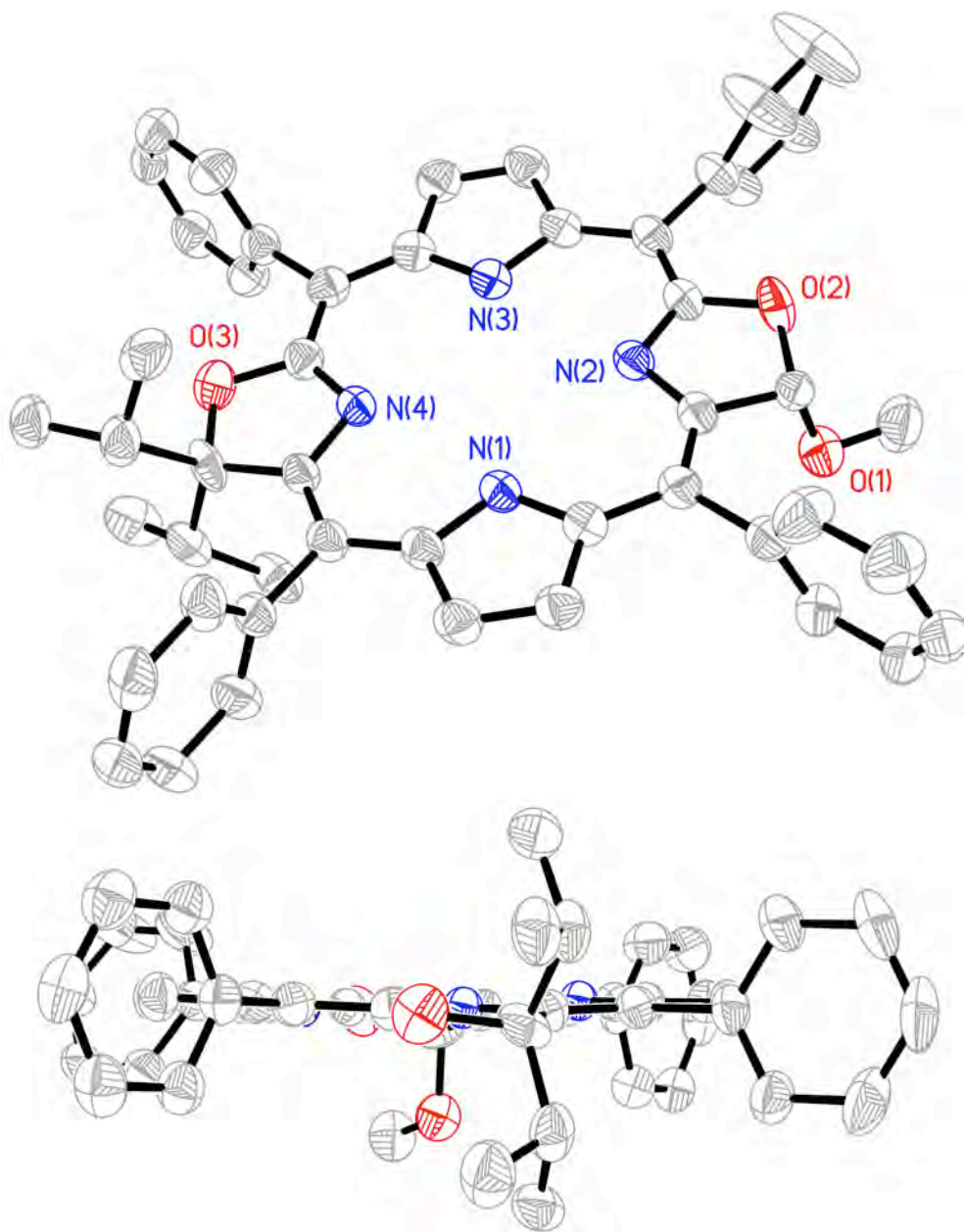


Figure 45. ORTEP Representation of the crystal structure of **22-cis** , side and top views. Hydrogen atoms and disorder removed for clarity.

Table S6. Crystal data and structure refinement for **22-cis**.

Identification code	22-cis	
Empirical formula	$C_{49}H_{44}N_4O_3$	
Formula weight	736.88	
Temperature	100(2) K	
Wavelength	1.54178 Å	
Crystal system	Monoclinic	
Space group	P2(1)/c	
Unit cell dimensions	$a = 20.3320(5)$ Å	$\alpha = 90^\circ$
	$b = 11.1841(3)$ Å	$\beta = 109.5870(10)^\circ$
	$c = 18.4019(5)$ Å	$\gamma = 90^\circ$
Volume	$3942.36(18)$ Å ³	
Z	4	
Density (calculated)	1.242 Mg/m ³	
Absorption coefficient	0.613 mm ⁻¹	
F(000)	1560	
Crystal size	$0.55 \times 0.42 \times 0.38$ mm ³	
Theta range for data collection	2.31 to 64.45° .	
Index ranges	$-23 \leq h \leq 22$, $-12 \leq k \leq 11$, $-20 \leq l \leq 19$	
Reflections collected	23323	
Independent reflections	6350 [R(int) = 0.0315]	
Completeness to $\theta = 64.45^\circ$	96.1 %	
Absorption correction	SADABS	
Max. and min. transmission	0.8006 and 0.7297	
Refinement method	Full-matrix least-squares on F ²	
Data / restraints / parameters	6350 / 6 / 585	
Goodness-of-fit on F ²	1.037	
Final R indices [I > 2 σ (I)]	R1 = 0.0825, wR2 = 0.2563	
R indices (all data)	R1 = 0.0904, wR2 = 0.2674	
Largest diff. peak and hole	1.341 and -0.423 e.Å ⁻³	